REMARKS

Claims 234-247 and 466-479 are all the claims pending in the present application.

Claims 1-233, 248-465 and 480-509 have been cancelled.

Claims 241 and 246 have been objected to.

The rejection of claims 234-247 and 466-479 have been maintained.

The Applicants traverse the rejections and request consideration.

As noted in the response filed March 18, 2003, all the pending rejections are based on

ILLIADAS, either standing alone or in combination with other references. As evidenced by the

database report from PubMed submitted along with the response filed March 18, 2003, the

ILLIADAS reference, though having a "received" date of January 2000, has a publication date

of June 2000.

The Applicants respectfully attach a Declaration under 37 C.F.R. § 1.131, executed by all

the inventors, swearing behind the ILLIADAS reference. In order to avoid duplication, the

Applicants refer to the exhibits filed along with the unentered Declaration of Dr. Zvia Agur filed

March 18, 2003. Specifically items 11 and 14 have been referred to. The Declaration and the

Exhibits referred to demonstrate a conception date of at least prior to June 2000 and continued

diligence until October 19, 2000, the filing date of the present application.

As noted in the Declaration, the applicants completed the invention prior to June 2000,

the date of publication of the ILLIADAS reference. Prior to June 2000, the Applicants conceived

the invention and conveyed the subject matter to the drafters of the relevant documents attached

to Dr. Agur's Declaration of March 2003.

Referring to the documents that were attached to the March 2003 Declaration of Dr. Zvia Agur, the Examiner incorrectly notes that the Applicants have not proven an earlier conception of the invention, at least that the Applicants have not proven the conception of several components of the invention.

The Applicants respectfully submit that the Examiner has not reviewed all the documents attached to the March 2003 declaration. The Applicants attach a claim chart of the pending claims specifically pointing out where in the documents submitted the requisite proof of conception can be found. It should be noted that this is only exemplary in nature and additional proofs can be found in several parts of the submitted documents in addition to the ones listed in the attached claim chart. For convenience, additional copies of items 11 and 14 have been attached herein with page numbers for a better understanding of the attached claim chart. It should also be noted that the designation x:y indicates page no. x and line y in the document referred to.

Therefore, the Applicants respectfully submit that ILLIADAS does not qualify as prior art under any sections of 35 U.S.C. § 102.

Considering the above, it is respectfully requested that the pending claims be passed into allowance and the Applicants be awarded what is believed to be their rightful due.

CONCLUSION

In view of the above, reconsideration and allowance of this application are now believed to be in order, and such actions are hereby solicited. If any points remain in issue which the Examiner feels may be best resolved through a personal or telephone interview, the Examiner is kindly requested to contact the undersigned at the telephone number listed below.

The USPTO is directed and authorized to charge all required fees, except for the Issue Fee and the Publication Fee, to Deposit Account No. 19-4880. Please also credit any overpayments to said Deposit Account.

Respectfully submitted,

Chidul- S Iyer

SUGHRUE MION, PLLC
Telephone: (202) 293-7060
Facsimile: (202) 293-7860

Chid S. Iyer
Registration No. 43,355

WASHINGTON OFFICE
23373
CUSTOMER NUMBER

Date: September 3, 2003

11

234.	A computer system for recommending an optimal treatment protocol for treating cancer using drugs, for an individual, said system interfacing with the computer and said system further comprising:	Item 11, page 70, lines 1-5 (hereinafter 70:1-5)
I	a cancer system model;	Item 11: 5:20-25, 58:20-59:10, 54:4-7 Item 14: 2:33-40
II	a treatment protocol generator for generating a plurality of treatment protocols for treating cancer using chemotherapy;	Item 11: 6:6-10, 64: 19-65:15, 72:15
III	a system model modifier, wherein said the system model modifier is adapted to modify said cancer system model based on parameters specific to the individual; and	Item 11: 6:1-3, 59:23-60:12, 63:7-14, 71:10-13, 72:5-7
IV	a selector adapted to select an optimal treatment protocol from said plurality of treatment protocols based on the modified system model.	Item 11:6:15-17, 66:7-68:25, 71:14-15
235.	The system of claim 234 wherein the system model further comprises:	
I	a process model of cancer development; and	Item 14: 13-15
II	a treatment model that is adapted to model the effects of treating cancer with drugs, including chemotherapy.	Item 11:71:7-9
236.	The system of claim 235 wherein said process model incorporates a distribution of cycling cells and quiescent cells.	Item 14: 3:14-16

237.	The system of claim 235 where a tumor cell cycle is divided into at least four compartments G1, S, G2 and M and a quiescent stage is denoted by G0, wherein each of said four compartments is further subdivided into sub-compartments and an ith sub-compartment representing cells of age I in the corresponding compartment, wherein the system is adapted to ensure that cells entering a compartment always enter a first sub-compartment of the compartment.	Item 14: 3:18-35
238.	The system of claim 237 wherein the model development of cancer cells using a predetermined set of parameters by calculating a number of cells in each subcompartment using stepwise equations.	Item 14: 4:15-30
239.	The system of claim 238 wherein the system is adapted to use a probability vector is used to determine a fraction of cells that leaves any subcompartment in a compartment to move to a first subcompartment of the next compartment.	Item 14: 3:30-35, 5:1-3
240.	The system of claim 238 where the system includes a set control functions that are adapted to uniquely determine an outcome of every single step, wherein said control functions comprise age of cells, state of a current population and associated environment.	Item 14: 5:4-12
241.	The system of claim 238 wherein the system comprises a model representing a tumor the model comprising a combination of a	Item 14: 5:18-20

2

	plurality of homogeneous groups of cells, each of said homogeneous groups of cells representing a similarly behaving group of cells distributed between all the cell-cycle compartments.	
242.	The system of claim 241, wherein the system is adapted to calculate in each step, a number of cells in each sub-compartment of each compartment of each group according to factors including a previous state, parameters of tumor, tumor current microenvironment and drug concentration.	Item 14:5:27-32
243.	The system of claim 242 where spatial structure of the tumor is included in the model.	Item 14:5:32
244.	The system of claim 243, wherein the system is adapted to incorporate pharmacokinetic and pharmacodynamic, cytostatic effects, cytotoxic effects, and other effects on cell disintegration of anticancer drugs.	Item 14:6:4-20
245.	The system of claim 244 wherein the system is adapted to incorporate a dose-limiting toxicity into the model.	Item 14:6:4-20, 7:4-20
246.	The system of claim 234 wherein, said parameters specific to the individual comprise parameters related to tumor dynamics, patient specific drug, pharmacodynamic and dynamics of dose-limiting host tissues.	Item 14:6:4-20, 7:4-20
247.	The system of claim 246, wherein said parameters related to tumor dynamics comprise age, weight, gender, percentage of limiting healthy cells,	Item 14:6:4-20, 7:4-20

	desired length of treatment protocol, previous reaction to treatment, molecular markers, genetic markers, pathologic specifics and cytologic specifics.	
466.	A computer-implemented method for recommending an optimal treatment protocol for treating cancer using drugs , including chemotherapy, for an individual, said method comprising:	Item 11, page 70, lines 1-5 (hereinafter 70:1-5)
I	creating a cancer system model;	Item 11: 5:20-25, 58:20-59:10, 54:4-7 Item 14: 2:33-40
II	enumerating a plurality of treatment protocols for treating cancer using drugs;	Item 11: 6:6-10, 64: 19-65:15, 72:15
III	modifying the system model based on parameters specific to the individual;	Item 11: 6:1-3, 59:23-60:12, 63:7-14, 71:10-13, 72:5-7
IV	selecting an optimal treatment protocol from said plurality of treatment protocols based on the modified system model; and	Item 11:6:15-17, 66:7-68:25, 71:14-15
V	recommending said optimal treatment.	Item 11:6:15-17, 66:7-68:25, 71:14-15
467.	The method of claim 466 wherein the system model further comprises:	
I	a process model of cancer development; and	Item 14: 13-15
II	a treatment model that models the effects of treating cancer with drugs, including chemotherapy.	Item 11:71:7-9
468.	The method of claim 467 wherein said process model incorporates a distribution of cycling cells and	Item 14: 3:14-16

	quiescent cells.	
469.	The method of claim 467 where a tumor cell cycle is divided into at least four compartments G1, S, G2 and M and a quiescent stage is denoted by G0, wherein each of said four compartments is further subdivided into sub-compartments and an ith sub-compartment representing cells of age I in the corresponding compartment, wherein cells entering a compartment always enter a first sub-compartment of the compartment.	Item 14: 3:18-35
470.	The method of claim 469 wherein the model traces development of cancer cells using a predetermined set of parameters by calculating a number of cells in each subcompartment using stepwise equations.	Item 14: 4:15-30
471.	The method of claim 470 wherein a probability vector is used to determine a fraction of cells that leaves any subcompartment in a compartment to move to a first subcompartment of the next compartment.	Item 14: 3:30-35, 5:1-3
472.	The method of claim 470 where a set control functions uniquely determine an outcome of every single step, wherein said control functions comprise age of cells, state of a current population and associated environment.	Item 14: 5:4-12
473.	The method of claim 470 wherein a tumor is modelled as a combination of a plurality of homogeneous groups of cells, each of said homogeneous groups of cells representing a similarly behaving group of cells distributed	Item 14: 5:18-20

	between all the cell-cycle compartments.	
474.	The method of claim 473, wherein in each step, a number of cells in each sub-compartment of each compartment of each group is calculated according to factors including a previous state, parameters of tumor, tumor current microenvironment and drug concentration.	Item 14:5:27-32
475.	The method of claim 474 where spatial structure of the tumor is included in the model.	Item 14:5:32
476.	The method of claim 475, wherein pharmacokinetic and [PD], cytotoxic effects, cytostatic effects and other effects on cell disintegration of anticancer drugs are incorporated into the model.	Item 14:6:4-20
477.	The method of claim 476 wherein a dose-limiting toxicity is incorporated into the model.	Item 14:6:4-20, 7:4-20
478.	The method of claim 466 wherein, said parameters specific to the individual comprise parameters related to tumor dynamics, patient specific drug, pharmacodynamic, and dynamics of dose-limiting host tissues.	Item 14:6:4-20, 7:4-20
479.	The method of claim 478, wherein said parameters related to tumor dynamics comprise age, weight, gender, percentage of limiting healthy cells, desired length of treatment protocol, previous reaction to treatment, molecular markers, genetic markers, pathologic specifics and	Item 14:6:4-20, 7:4-20

		cytologic specifics.	

IN THE UNITED STATES PATENT AND TRADEMARK OFFICE

In re application of

Docket No: Q60688

Zvia AGUR, et al.

Appln. No.: 09/691,053

Group Art Unit: 1631

Confirmation No.: 5359

Examiner: Marjorie A. MORAN

Filed: October 19, 2000

For: SYSTEM AND METHOD FOR OPTIMIZED DRUG DELIVERY AND PROGRESSION OF DISEASED AND NORMAL CELLS

DECLARATION UNDER 37 C.F.R. § 1.131

Honorable Commissioner of
Patents and Trademarks
Washington, D.C. 20231

Sir:

We, Zvia Agur, Sarel Fleishmann, Kirill Skomorovski and Moshe Vardi hereby declare as follows:

We are inventors and applicants of the invention entitled "System and Method for Optimized Drug Delivery and Progression of Diseased and Normal Cells", disclosed and claimed in U.S. Application No. 09/691,053 filed October 19, 2000.

Prior to June 2000, we had invented the invention as described and claimed in the above-identified application, and pursued the present invention in the ordinary course of business.

The entire inventive work was done in Israel.

Prior to June 2000, we met with and conveyed the entire subject matter of the invention to the drafters of the documents included in Appendix A of the 1.131 declaration by Dr. Zvia Agur submitted to the USPTO on March 18, 2003. Specifically, the information conveyed by us prior to June 2000, also includes those appearing in items 11 and 14 of
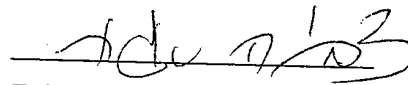
Appendix A of the 1.131 declaration by Dr. Zvia Agur submitted to USPTO on March 18, 2003.

The above-identified application was prepared based on the documents included in Appendix A of the 1.131 declaration by Dr. Zvia Agur (submitted on March 18, 2003). The above-identified application was then filed on October 19, 2000.
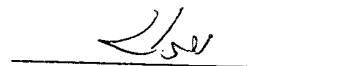
In view of the discussion above, we had invented the claimed invention disclosed in the subject application prior to June 2000, and pursued the present invention in the ordinary course of business, including preparing the above-identified patent application, until the application was filed on October 19, 2000.

We declare further that all statements made herein are of our own knowledge and are true and that all statements made on information and belief are believed to be true; and further that these statements were made with the knowledge that willful false statements and the like so made are punishable by fine or imprisonment, or both, under Section 1001 of Title 18 of the United States Code, and that such willful false statements may jeopardize the validity of the application or any patent issuing thereon.
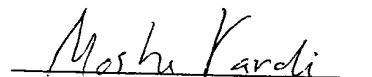
Date: 1.8.03

Zvia Agur

Date: 1.8.03

Sarel Fleishmann

Date: 1.08.03

Kirill Skomorovski

Date: 1.08.03

Moshe Vardi

IN THE UNITED STATES PATENT AND TRADEMARK OFFICE

In re application of

Zvia AGUR, et al.

Appln. No.: 09/691,053

Confirmation No.: 5359

Filed: October 19, 2000

Docket No: Q60688

Group Art Unit: 1631

Examiner: Marjorie A. MORAN

For: SYSTEM AND METHOD FOR OPTIMIZED DRUG DELIVERY AND PROGRESSION OF DISEASED AND NORMAL CELLS

DECLARATION UNDER 37 C.F.R. § 1.131

Honorable Commissioner of
Patents and Trademarks
Washington, D.C. 20231

Sir:

We, Zvia Agur, Sarel Fleishmann, Kirill Skomorovski and Moshe Vardi hereby declare as follows:

We are inventors and applicants of the invention entitled "System and Method for Optimized Drug Delivery and Progression of Diseased and Normal Cells", disclosed and claimed in U.S. Application No. 09/691,053 filed October 19, 2000.

Prior to June 2000, we had invented the invention as described and claimed in the above-identified application, and pursued the present invention in the ordinary course of business.

The entire inventive work was done in Israel.

Prior to June 2000, we met with and conveyed the entire subject matter of the invention to the drafters of the documents included in Appendix A of the 1.131 declaration by Dr. Zvia Agur submitted to the USPTO on March 18, 2003. Specifically, the information conveyed by us prior to June 2000, also includes those appearing in items 11 and 14 of
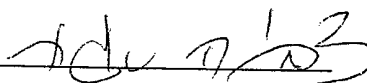
Appendix A of the 1.131 declaration by Dr. Zvia Agur submitted to USPTO on March 18, 2003.

The above-identified application was prepared based on the documents included in Appendix A of the 1.131 declaration by Dr. Zvia Agur (submitted on March 18, 2003). The above-identified application was then filed on October 19, 2000.

In view of the discussion above, we had invented the claimed invention disclosed in the subject application prior to June 2000, and pursued the present invention in the ordinary course of business, including preparing the above-identified patent application, until the application was filed on October 19, 2000.

We declare further that all statements made herein are of our own knowledge and are true and that all statements made on information and belief are believed to be true; and further that these statements were made with the knowledge that willful false statements and the like so made are punishable by fine or imprisonment, or both, under Section 1001 of Title 18 of the United States Code, and that such willful false statements may jeopardize the validity of the application or any patent issuing thereon.
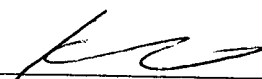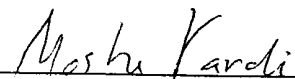
Date: 1.8.03

Zvia Agur

Date: 1.8.03

Sarel Fleishmann

Date: 1.08.03

Kirill Skomorovski

Date: 1.08.03

Moshe Vardi

FIELD OF THE INVENTION

The present invention relates to a system and method for predicting and optimization of treatment of disease and of certain stages in drug development and trials.

BACKGROUND OF THE INVENTION

Drugs that are administered to combat disease are often toxic to healthy cells as well. In prescribing a treatment protocol, it is necessary to consider the effect of the protocol on both abnormal and normal cells.

Mathematical models of biological systems are well known in the art. As a broad category, these models are...

More specifically, can have models of cell lines, tumor growth, etc. Use of these models for prediction of treatment results is also known in the art. However, predictive models generally employ an analytical approach, in which generalizations about the use of the treatment on a disease must be made. This approach, while providing useful general information, cannot be used to predict results of treatment in realistic circumstances. Thus, a method which is inclusive of more complex and detailed scenarios is needed.

SUMMARY OF THE INVENTION

To be completed when claims are finalized.

2

BRIEF DESCRIPTION OF THE DRAWINGS

The present invention will be understood and appreciated more fully from the following detailed description taken in conjunction with the appended drawings in which:

Fig. 1 is a schematic illustration of the basis of the present invention;

Fig. 2 is a flow chart illustration of steps of the invention, useful in understanding Fig. 1;

Fig. 3 is a schematic illustration of a biological model, in accordance with one embodiment of the present invention;

Fig. 4 is a chart illustration of the biological model of Fig. 3;

Fig. 5 is a graphical illustration of the chart of Fig. 4;

Fig. 6 is a chart illustration of the biological model of Fig. 3 in a different format;

Fig. 7 is a graphical illustration of the chart of Fig. 6;

Figs. 8A and 8B are graphical illustrations of the output of the model of Fig. 3;

Figs. 9A and 9B are graphical illustrations of experimental data as compared to the output shown in Figs. 8A and 8B;

Fig. 10 is a schematic illustration of a biological model, in accordance with a further embodiment of the present invention;

Fig. 11 is a graphical illustration of results of the simulation of the model shown in Fig. 10;

Figs. 12A and 12B are graphical illustrations of the effects of two doses of G-CSF on the neutrophil line, according to the model of Fig. 10;

3

Fig. 13 is a schematic illustration of a biological model, in accordance with a further embodiment of the present invention;

4

DETAILED DESCRIPTION OF THE PRESENT INVENTION

A system and method have been developed for identifying optimal treatment protocols for selected parameters. Unlike prior art optimization schemes, the present invention uses heuristic determinations. The use of heuristics enables to find near optimal solutions even for complex (hence, realistic) mathematical descriptions of the relevant biological/clinical/pharmacological scenarios; this holds both for the general case ("optimal generic treatment"), as well as at the level of an individual patient. Reference is now made to Fig. 2, which is a flow chart illustration generally showing the optimization method. The Figure generally depicts the basic concept. The present invention optimizes a drug delivery protocol after consideration of possible protocols, referred to as a protocol space. Determination of optimal protocol is based on specific parameters input by a user. The user may be a physician, a drug developer, a scientist, or anyone else who may need to determine a treatment protocol for a drug. The specific parameters may include several categories, such as individual patient characteristics and/or medical history, needs of a specific user (research, efficacy, treatment, etc.), and other particulars (such as maximum length of treatment, confidence level, etc.).

The first steps include generation of several types of models. A set of models for all the relevant biological processes, is created. In addition, a model of treatment effects on each of these processes is created. The combination of these models provides a detailed mathematical model of the overall bio-clinical scenario in a general or specific sense together with the specific effects of a particular treatment. Once the comprehensive model is

5

constructed the characteristic parameters (either population averaged or patient specific e.g., – age, gender, weight or clinical indications) are implemented in it. In this way a "virtual" patient is generated.The next step is definition of a protocol space. To do this, possible permutations of certain

5   parameters such as drug doses, dosing intervals, drug quantity, etc. are considered. Thus, a number (can be very large) of possible treatment protocols is generated. The amount of possibilities depends on the number and ranges of parameters considered. At this point, the fitness function is constructed by mathematically considering different possible factors which

10 may be influenced by the treatment. These may include survival, tumor or pathogen load, cytotoxicity, side effects, pain etc. The user can put certain specific parametersin the fitness function so as to adjust this function to his/her specific goalsBased on the selected parameters, the fitness function is applied, and calculates a fitness score for each and every possibility in the

15 protocol space. Finally, the optimization step is carried out, either by search heuristics or by **analytical methods**, in order to select the optimal treatment protocol from all the scored possibilities.

In this way, a disease specific, patient specific, situation specific, drug specific, objective specific treatment protocol may be obtained. The actual

20 time it takes once the parameters are entered may be negligibly short or up to hours, depending on the length of the simulated treatment period and the power of the specific search heuristics and the computational tools, making this a very feasible tool.

Construction of detailed mathematical models for biological processes

25 and treatments will be shown by way of example. A model of platlets

10

production and thrombocytopeniawith treatment by TPO, a model of neutrophil production and neutropenia and treatment by G-CSF, and a model of cancer growth and chemotherapy are described. An example for specific optimization (by linear programming) is implemented in the neutrophil model. A general heuristic optimization method is described as well.

EXAMPLE 1:Thrombocytopenia and Treatment by Thrombopoietin (TPO)

Thrombocytopenia is a common hazardous blood condition, which may appear in different clinical situations, including cancer chemotherapy. Recently, a thrombopoiesis-controlling cytokine, thrombopoietin (TPO), was isolated and its human recombinant analog became available. A mathematical model has been developed to imitate dynamics of a thrombopoietic lineage in the bone marrow, of platelet counts in the periphery, and effects of TPO administration on them **[on what? Platelets?]**.

TPO is a cytokine, glycoprotein of about 350 amino acids, that resembles erythropoiesis-stimulating hormone, erythropoietin. Its synthetic analogs, recombinant human thrombopoietin (rHuTPO) and recombinant human megakaryocyte growth and development factor (rHuMGDF), are available as well and are undergoing clinical trials. These compounds have been shown to have the same biological activity as TPO has, so the term TPO will be used without distinguishing between its different forms and analogs.

TPO is a primary growth factor of the thrombopoietic cell line both *in vivo* and *in vitro*. Aside from this, TPO may be potent in stimulation and co-

7

stimulation of other hemopoietic lineages (e.g., granulopoietic or erythropoietic).

I. MODEL OF BIOLOGICAL SYSTEM

A. Background of Thrombopoiesis

5   Like all other hemopoietic lines, the thrombopoietic line originates from poorly differentiated, multipotential cells, capable of some division and self-reconstitution. Other bone marrow cell lines, such as pluripotential hemopoietic stem cells and common myeloid progenitor cells (CFU-GEMM) have these characteristics as well.

10   Starting out as undifferentiated stem cells, the cells gradually become more and more differentiated and committed to a specific line. Once they commit to the thrombopoiesis line, they proliferate extensively within certain compartments. One such compartment is that of colony-forming units – megakaryocytes (CFU-Meg). Other examples of compartments burst-forming

15   units – megakaryocyte (BFU-Meg) and megakaryoblast compartments, which have similar properties as one another.

         The committed thrombopoietic cells, which are megakaryocyte precursors, go through several stages of maturation when proliferation is no longer possible. However, megakaryocyte maturation is somewhat different

20   from maturation within other hemopoietic lines. In megakaryocytes, cell nuclei undergo mitosis in parallel with cytoplasmic maturation. However, although the DNA material of these cells doubles, cell division does not happen. Such incomplete mitosis is called endomitosis. Consequently, the cell becomes

polyploid with 2N, 4N, 8N, etc., amounts of DNA. The cells with 2N to 4N chromosomes are called either megakaryoblasts or megakaryocytes.

Usually, megakaryocytes do not start to release platelets until the 16N state. Then they begin to create demarcation membranes that envelop cytoplasm fragments **generating platelets [what does this refer to?]**. The platelets are then released into the blood stream. The amount of cytoplasm, cell volume and an ability to release platelets all increase proportionally to the cell ploidy.

B. Mathematical Model

Reference is now made to Fig. 3, which is a detailed illustration of a model predicting thrombopoiesis. As shown in Fig. 3, the thrombopoietic lineage is divided into eight compartments. The first compartment, called Stem Cells (SC) and labeled 30, refers to all bone marrow hemopoietic progenitors that have an ability to differentiate into more than one line (e.g., pluripotential stem cells, CFU-GEMM, and others). Cells of SC compartment 30 proliferate, mature, and subsequently differentiate into megakaryocytes or other precursors, or they may give rise to new stem cells. Although the term "new" is not biologically accurate, it serves as an acceptable assumption for the purposes of the model.

Cell death through apoptosis may have a significant effect on cell number within proliferating compartments. However, the effect of apoptosis is combined with the effect of cell proliferation into a total amplification of cell number in a given compartment. Thus, for example, the amplification rate of cells in SC compartment 30 is normally 1.029 new cells per hour. An

assumption is made that no apoptosis occurs in non-proliferating megakaryocytic compartments, due to lack of evidence to the contrary.

Biologically, rates of proliferation and maturation, the ability to reconstitute, and other characteristics differ between particular cell types within a primitive progenitor population. However, in this model there is no distinction between them; all progenitor cells are considered to be one population with common properties.

Based on some works **[which ones?]** that have shown that probabilities of stem cell differentiation into one or another hemopoietic lineage are constant, it is assumed that a flow of stem cells into the megakaryocyte lineage depends only on the number of mature stem cells. The same was assumed about the stem cell self-renewal. Thus, after the cells spend a defined transit time, for example 24 hours, in SC compartment 30 a certain constant fraction of the cells (0.5181) return to their "young state", i.e. start their passage through SC compartment 30 again, as shown in line 31. Another constant fraction (0.342, for example) of cells pass into the next compartment called Colony-Forming Units (CFU-Meg), labeled 40. It is presumed that remaining stem cells differentiate into other hematopoietic lineages.

CFU-Meg refers to all cells that are already committed to the megakaryocyte line but are still capable of proliferation. Cells of CFU-Meg compartment 40, like those of SC compartment 30, spend some time (normally 60 hours) multiplying at an amplification rate of about 1.0255 **[per**

what?] and maturing before losing their proliferative abilities and passing on to the next compartment 50, called megakaryoblasts (MKB).

MKB compartment 50 includes all the cells that have lost the ability to proliferate, but are not yet sufficiently mature to release platelets. For the purposes of the model, the assumption is made that megakaryocytes do not start to release platelets until they reach the 16N-ploidy phase. Hence, MKB refers to 2N, 4N and 8N cells of megakaryocyte lineage that cannot divide, at all stages of cytoplasmic maturity. After these cells spend the designated transit time (normally 132 hours) in MKB compartment 50, they move to the next compartment 60, which is an MK16 bone marrow compartment.

The cells of MK16 compartment 60 are megakaryocytes of 16N-ploidy class that release platelets until they exhaust their capacity, and then are disintegrated. Cell volume has a linear relationship with megakaryocyte ploidy. Hence, we assume that all 16N-megakaryocytes have the same volume and, thus, the same platelet-releasing capacity. Therefore all platelet-releasing 16N-megakaryocytes are in transit for the same amount of time (120 hours) until they are exhausted and disintegrated.

However, some 16N-megakaryocytes do not participate in platelet release, but rather continue with another endomitosis over a 48-hour time period, and become 32N-megakaryocytes. These constitute a new and distinct MK32 compartment 70. Thus, after 48 hours in MK16 compartment 60, a certain fraction of the cells (normally 0.26) leave MK16 compartment 60 and go on to MK32 compartment 70.

32N-megakaryocytes release platelets as well. The rate of platelet release is constant for every compartment and proportional to the ploidy state of megakaryocytes in it. Thus, every 16N-megakaryocyte releases 10.2 platelets per hour and every 32N-megakaryocyte releases 20.4 platelets per

5 hour. However, 32N-megakaryocytes are not exhausted more quickly than 16N-megakaryocytes, since they have 2 times greater volume and platelet-releasing capacity. Consequently, all platelet-releasing megakaryocyte compartments have the same transit time.

Once again, some fraction of cells (normally 0.016) are not engaged in

10 platelet formation, and continue to the 64N-stage. Additional endomitosis in MK32 compartment 70 takes the same amount of time (48 hours) as in MK16 compartment 60. The 64N-megakaryocytes continue the process in a new MK64 compartment 80, and 0.4 of them become 128N-cells in yet another MK128 compartment 90. Additional endomitosis in MK64 compartment 80

15 takes the same amount of time (48 hours) as before.

Normally, 64N- and 128N-megakaryocytes are not found in humans. However, these cells were detected in human bone marrow in some abnormal conditions. Therefore, we included these compartments in our model, but in the normal state their number is negligible. As far as we know,

20 megakaryocytes of greater ploidy classes have not been encountered in humans.

Finally, there is a platelet compartment 100. This is not a bone marrow compartment, but rather the platelet pool in the peripheral blood **[(spleen sequestration???)]**. Platelets released from megakaryocytes of 16N-, 32N-,

12

64N-, and 128N-ploidy classes enter platelet compartment 100. Platelet elimination from the blood is presumed to occur after a defined transit time in circulation by a mechanism of death from senescent **[what is this?]**. To simplify the model we ignore the destruction of platelets by their use **[?]**.

5 Transit time through platelet compartment 100 is 240 hours but can vary, as will be discussed below.

II. MODEL OF TREATMENT EFFECTS

A. Background of TPO

The major sites of TPO production are the liver and kidney. TPO is also

10 produced in the spleen and bone marrow, but the production rate in these organs is 5 times lower than in the liver and kidney. Some low TPO production has also been found in many other sites in the body. Rates of liver and kidney TPO production are constant under thrombocytopenia and thrombocytosis of varying degrees of severity. TPO production in the spleen

15 and bone marrow is inversely related to the megakaryocyte mass, but the actual contribution is negligible with regard to total TPO production.

Another mechanism of TPO concentration regulation is receptor-mediated TPO uptake, since TPO-receptors on the platelet and megakaryocyte surfaces are the main TPO-clearance mechanism. Thus,

20 TPO concentration is inversely related to the total platelet and megakaryocyte mass.

The effects of TPO on the thrombopoietic line may be divided into three types: (i) stimulation of proliferation of megakaryocyte progenitors that have

13

an ability to proliferate; (ii) stimulation of maturation of all megakaryocyte progenitors; (iii) induction of additional endomitosis of already mature megakaryocytes, which leads to an increase in the modal megakaryocyte ploidy.

B. Mathematical Model of TPO Effects

TPO concentration effects on the thrombopoiesis line is now considered. As discussed above, three things depend on TPO concentration: (i) amplification rate (amp), (ii) the rate of cell maturation or, alternatively, transit time through a given compartment (transit), and (iii) the fraction of megakaryocytes of given ploidy that undergo additional endomitosis and pass on to the next ploidy class.

<u>1. TPO Concentration</u>

Recombinant human full-length TPO and its truncated form rHuMGDF are fully active biologically. Therefore, in our model we add exogenously administered recombinant protein to endogenously produced TPO in order to calculate actual TPO concentration.

As mentioned above, the rate of TPO production in the main TPO production sites, i.e. liver and kidney, is constant under thrombocytopenia or thrombocytosis. The level of TPO mRNA in sites like the bone marrow and spleen, where it is produced in a 5-fold lower rate than in the liver and kidney, is not significantly different from the TPO level in peripheral blood. Therefore, the assumption is made that the bone marrow and spleen contributions to the total TPO concentration are insignificant. Endogenously produced TPO is

assumed to have a constant rate of production of 7 pg/ml/hour. However, this number can change.

5   The main mechanism that controls TPO concentration in the blood is receptor-mediated TPO uptake. Both megakaryocyte and platelet mass contribute to the total receptor number (normally 8.375×10^9) and, consequently, to the rate of TPO clearance. We assume that every platelet bears 220 TPO receptors **[based on what?]**. Each megakaryocyte at any given moment bears an amount of receptors equal to the number of platelets

10   that can be released during the remaining life-span, times 220 receptors per potential platelet. We assume also that every receptor molecule removes 4.776×10^{-10} pg/ml/hour of TPO from circulation. However, this number can change.

       Another mechanism of TPO removal from the blood is non-specific

15   TPO-receptor-independent clearance. This mechanism is rather insignificant in the normal state, when receptor-mediated TPO binding, endocytosis, and degradation remove most of the TPO. However, when the amount of TPO rises significantly above the ability of the receptor pool to remove it, non-specific clearance becomes important. In our model this type of TPO

20   clearance is exponential, i.e. every hour some fraction (0.03) of a current amount of TPO is removed from circulation.

       Exogenous TPO is included in the model as a linear relation of the initial maximum TPO blood concentration to the administered intravenous (IV) dose (the relation coefficient is 0.0167) based on literature data.

15

The state when TPO completely disappears from the blood is very unlikely, the lower limit of possible TPO concentration is restricted to a certain minimum, in this case 0.01 pg/ml.

Thus, the formula that calculates TPO concentration hourly is given in Equation 1 as follows:

$$C_{i+1} = \max\left((C_i + Endo + 0.0167 \cdot Exo - Nc \cdot C_i - Rc \cdot Rp), 0.01\right) \quad (1)$$

where C_i is TPO concentration at the current hour (i), C_{i+1} is TPO concentration at the next hour, Endo is endogenously produced TPO per hour, Exo is the total amount of TPO administered intravenously during the current hour, Nc is the coefficient of non-specific TPO clearance, Rc is the coefficient of receptor-mediated TPO clearance, i.e. amount of TPO that each receptor removes per hour, and Rp is the total TPO-receptor pool.

In steady-state TPO concentration is constant and equals 100 pg/ml.

2. TPO effects on amplification rate

In our model, there are only two compartments, SC compartment 30 and CFU-Meg compartment 40, whose cells are capable of dividing. These compartments differ significantly from each other, so they will be discussed separately. Cells of other compartments do not proliferate, so their amplification rate equals 1 under all circumstances.

a. SC compartment 30:

Cells of SC compartment 30 are relatively insensitive to TPO as compared to committed megakaryocytic cells. In our model this is considered

as a threshold of 2500 pg/ml of TPO concentration, but this number can be changed. TPO affects stem cells only above this concentration. As long as TPO remains below the threshold, stem cells are regulated by an intrinsic TPO-independent mechanism that keeps the size of their population almost

5   constant.

Thus, below the threshold, SC amplification rate (amp_{SC}) is determined hourly depending on the current number of cells in SC compartment 30. The dependence equation gives a sigmoidal function: amp_{SC} changes from 1 (i.e., no amplification, the cell number remains the same) up to the maximal value

10   when the cell number approaches infinity or 0, respectively **[??]**. When the cell number is normal **[define normal]** amp_{SC} equals one fourth of its maximal possible value. Stem cell amplification rate is defined by Equation 2 as follows:

15
$$amp_{SC}(quant_{SC}) = (amp_{SC\,max} - 1) \cdot \frac{quantnorm_{SC}^{\,S}}{3 \cdot quant_{SC}^{\,S} + quantnorm_{SC}^{\,S}} + 1 \qquad (2)$$

where amp_{SCmax} is the maximal possible rate of cell amplification in SC compartment 30, $quantnorm_{SC}$ is the normal quantity of cells in SC

20   compartment 30, $quant_{SC}$ is an actual quantity of cells there, and S is a value that determines the sensitivity of the mechanism that links the amplification rate to the number of cells. A high value for S means that amp_{SC} changes significantly due to silent changes of $quant_{SC}$, and a low value for S means that amp_{SC} remains relatively constant whatever the changes of $quant_{SC}$ may

25   be. S generally equals 0.2, but this number can be changed.

In a range of very low cell numbers (100 times lower then normal or less), the model must define the stem cell parameters for the quickest recovery of SC compartment 30. Thus, amp_{SC} in these conditions achieves the maximal value (amp_{SCmax}).

5   On the other hand, the rise of TPO concentration above the threshold should occur in severe platelet and/or megakaryocyte deficiency, or when TPO has been administered exogenously. In these situations the hemopoietic system mobilizes additional resources for recovery of platelets and platelet-releasing compartments.   Hence, we assume that in an effective

10   concentration, TPO increases the rate of cell amplification in SC compartment 30. This is shown in Equation 3, as follows:

$$amp_{SC}(quant_{SC}, C_i) = \left((amp_{SC\,max} - 1) \cdot \frac{quantnorm_{SC}^{s}}{3 \cdot quant_{SC}^{s} + quantnorm_{SC}^{s}} + 1 \right) + (amp_{SC\,max} - 1) \cdot F^{*}\!\left(G^{*}(C_i - thres), St\right) \quad (3)$$

15

where the first of two operands is the amplification calculated based on a TPO-independent mechanism, and the second is the TPO-related addition to the amplification rate.

          G^{*} is a function that transforms concentration (C) into a form that is

20   easy to use in the calculation of both amp_{SC} and $transit_{SC}$ as will be discussed futher **[where?]**. G^{*} is defined by Equation 4 as follows:

$$G^{*}(C) = \ln(C + 1) \cdot 0.23 + 0.03949 \quad (4)$$

25

F^{*} in Equation 3 is a function that determines the steepness, denoted St, of the amp_{SC}-versus-C_i curve. F^{*}, as shown in Equation 5, is a recurrent function

18

that adds 1 to its first argument and applies a logarithm to this sum. Thereafter, 1 is added another time and a logarithm is applied to the sum again. This operation is repeated St times.

5

$$\mathbf{F}^*\left(x\right) = \ldots \log\left(\log\left(\log\left(\log\left(x+1\right)+1\right)+1\right)+1\right)\ldots \quad (5)$$

Although St appears in several equations, its value is specific for every case. In Equation 3, $thres$ is the threshold above which TPO has an effect on the

10 cells. In order to avoid an abrupt change of amp_{SC} when TPO concentration transcends the threshold, the TPO-related addition is calculated relative to the difference between an actual TPO concentration and the threshold.

b. CFU-Meg Compartment 40:

15

In contrast to the cells of SC compartment 30, cells of CFU-Meg compartment 40 are very sensitive to TPO and respond to the absolute TPO concentration, rather than its level above a certain threshold. Biologically, these cells have no TPO-independent proliferation mechanism, and thus

20 cease to proliferate when deprived of TPO. However, in our model, CFU-Meg cells continue to proliferate without TPO at almost the same rate as with TPO. With normal TPO concentrations, amp_{CFU} equals one eighth of its maximal possible value (amp_{CFUmax}). The equation that describes the relation of amplification rate of CFU-Meg cells (amp_{CFU}) to TPO concentration (C_i) is:

25

$$amp_{CFU}\left(C_i\right) = \left(amp_{CFU\,max} - 1\right)\cdot \mathbf{F}\left(\mathbf{G}\left(C_i\right), St\right) + 1 \quad (6)$$

Function **G** resembles function **G**[*] (Equation 4) qualitatively but differs quantitatively, having the following form:

$$G(C) = 2.56 \times 10^{-6} \cdot \left(\ln(C+1) + 0.3949\right)^7 + 0.3 \qquad (7)$$

Function **G** is changed from function **G**[*] by adding 0.3949, raising to a power of 7, multiplying by 2.56×10^{-6}, and adding 0.3. These changes provide the following features:

(a)   in the region near the normal TPO concentrations the function rises with an increasing rate from about 0.3 up to about 0.8;

(b)   in the normal TPO concentration (100 pg/ml) it equals 0.5;

(c)   in high TPO concentrations, which occur in cases of exogenous TPO administration, the function rises with a decreasing rate;

(d)   despite (iii), in high TPO concentrations that may arise in a logical situation (i.e. severe thrombocytopenia or TPO administration in logical doses), the rate of function growth does not drop down to zero and the function does not reach a maximum, but rather the rate gradually stabilizes at a nearly constant value and the function continues to rise almost linearly.

Function **F** in Equation 6 is almost the same function as function **F**[*] in Equation 5. The difference is that while **F**[*] returns the number solely on the basis of Equation 3, **F** is required to return to 0.5 when its first argument is 0.5, no matter what *St* is. This is achieved by multiplying the returned number by a certain coefficient, which is specific for every value of *St*. Thus, F is defined by Equation 8 as follows:

20

$$\mathbf{F}(x) = k \cdot \left(\ldots \log \left(\log \left(\log \left(\log \left(x + 1 \right) + 1 \right) + 1 \right) + 1 \right) \ldots \right) \qquad (8)$$

where k is the St-specific coefficient.

5

3. TPO effects on transit time

As noted earlier, all platelet-releasing megakaryocyte compartments have the same transit time. Since neither the relationship of megakaryocyte

10   volume (and thus, its platelet releasing capacity) to megakaryocyte ploidy, nor its rate of platelet release, are affected by TPO, the transit time through the compartments are constant, for example 120 hours. Platelets in circulation also spend constant period of time (eg. 120 hours) which is not affected by TPO concentration.

15   In contrast, SC, CFU-Meg, and MKB compartments have changeable transit times. If the transit time were continuously strictly related to the TPO concentration, then during an abrupt concentration change (in exogenous administration, for example) there could be either massive cell exit from the given compartment or absolute absence of cell exit for the period of time that

20   equals the difference between current and previous transit time. Since this situation seems biologically unlikely, in the present model transit time changes gradually, approaching the value that it should be equal to based on TPO concentration step by step.

Regarding the amplification rate, transit time in SC compartment 30

25   differs from the other compartments.

a. SC compartment 30:

Cells of this compartment respond to TPO only when its concentration rises above the threshold. Below the threshold stem cell transit time is regulated by an intrinsic mechanism dependent on the current cell number only. The value that the transit time should approach is determined based on the cell number, according to the following equation [=?]:

$$\blacksquare \tag{9}$$

where $transit_{SCmin}$ is the minimal possible transit time through SC compartment 30 (12 hours). It is two-fold lower than the normal transit time.

Unless the value that transit time should approach does not differ from the current transit time by more than 1.0, transit time does not changes. When it does differ, the transit time begins to change every hour by 1 hour in the direction of the value. [explain??]

When TPO concentration rises above the threshold, it sets the value which stem cell transit time approaches, to the following number [=?]:

$$\blacksquare \tag{10}$$

where $\mathbf{G}^*$ is the function given in Equation 4, C_i is the actual TPO concentration and *thres* is the same threshold as for stem cell amplification rate. Thus, TPO shortens stem cell transit time, which allows for the quickest recovery of committed megakaryocyte compartments when those **[what?]** are diminished. **[?]**

We assume maximal possible transit time (300 hours), above which transit time does not rise.

As in amplification rate, in a range of very low cell numbers (100 times lower then normal or less), the model must define the stem cell parameters for the quickest recovery of SC compartment 30. Thus, $transit_{SC}$ in these conditions achieves the maximal value, which is 300.

b. CFU-Meg and MKB compartments:

Transit times of these CFU-Meg and MKB compartments 40 and 50 are completely dependent on TPO concentration. The value, which the transit time approaches, is [=?]:

$$\times \tag{11}$$

where $transit_{(CFU-Meg/MKB)\ min}$ is the minimal possible transit time through CFU-Meg compartment 40 (eg. 30 hours) or MKB compartment 50 (66 hours), respectively. **G** is given in Equation 7, and **F** is the same function as in Equation **(7 or 8??)**, but the value of St is different in each equation. Maximal possible transit time is 100 hours for CFU-Meg compartment 40 and 350 hours for MKB compartment 50.

4. TPO effects on cell flow from one compartment to another

Cell flow between compartments refers not to the rate of cell passage from one compartment to the next, and not to the number of cells that pass

during a time unit, but rather to the proportion of "mature" cells that pass to the next compartment at any given moment, designated "*flowon*". "Mature" cells are ones that are potentially ready to pass to the next compartment but do not necessarily pass.

5   As was noted earlier, it is assumed that the fraction of SC compartment 30 that commits to the megakaryocytic lineage is constant (0.342) and TPO-independent. From the two following compartments, CFU-Meg compartment 40 and MKB compartment 50, every mature cell emerges to the next compartment regardless of external circumstances **[is this correct? Or just**

10 **TPO circumstances?]**. Thus, TPO does not affect the *flowon* in the first three compartments.

In contrast, the fraction of MK16-, MK32-, and MK64- megakaryocytes that continue with additional endomitosis and flow to the next compartment may change from almost 0 up to 1 depending on TPO concentration.

15 Because there is no compartment with ploidy greater than 128N, the megakaryocytes of MK128 compartment 90 do not flow to any other compartment, so there is no *flowon* value for MK128 compartment 90.

The dependence of MK16, MK32, and MK64 *flowon* parameters on TPO concentration is expressed by the following bi-phasic function:

20

$$\rule{8cm}{0.8cm} \tag{12}$$

25 where *flowonnorm* is the value of *flowon* under normal TPO concentration (100 pg/ml). This value for MK16 is 0.26, for MK32 it is 0.016, and for MK64 it is 0.4.

G° is a function that resembles the function **G** in Equation 7. The difference is that **G°** relates to the TPO concentration before a certain period of time rather than to the current TPO concentration. The reason for this is that it is assumed that a cell that enters a given megakaryocyte compartment

5   first "decides" whether to undergo additional endomitosis and not participate in platelet release in this compartment, or whether to begin with platelet release and remain in this compartment until complete exhaustion. TPO-dependent determination of what fraction of cells will "choose" each possibility occurs at the start of the cells' path through the given compartment. However,

10   the result of this determination can be seen when the cells that "decide" to leave the compartment actually leave it, i.e. after they complete one endomitosis. Thus, the fraction of cells that pass to the next compartment, *flowon*, is calculated based on the TPO concentration that existed before the period of one endomitosis (48 hours):

15

$$\rule{6cm}{0.4cm}$$

(13)

The time needed for additional endomitosis is the same in all three

20   compartments, MK16, MK32, and MK64.

III. COMPLETE DETAILED MODEL

The complete model was built as an imitation of what happens in real bone marrow. Each compartment is subdivided into small sections that contain the cells of a specific age with a resolution of one hour. For example,

25   the fifth age-section of MKB compartment 50 contains cells within MKB

25

compartment 50 that have been within that compartment for 5 hours. Every hour, all the cells in the "bone marrow" pass to the next age-section in the same compartment.

When the cell has spent all the transit time predetermined for it in a given compartment, it passes to the next compartment to the zero age-section. Thus, every hour the cells that leave one compartment fill the zero age-section of the next one. The cells that leave MK128 compartment 90 have nowhere to go and therefore disappear. The zero age-section of SC compartment 30 is filled by a certain fraction (0.5181) of the cells that leave SC compartment 30.

The cells that release platelets add a certain platelet number to the zero age-section of PL compartment 100 every hour.

Reference is now made to Fig. 4, which is an illustration of the implementation of the model. The model is implemented as a chart of 8 rows and 360 columns. The 8 rows relate to 8 cell compartments, and the columns relate to the age sections, with the assumption that transit time does not exceed 360 hours. This chart is updated hourly according to the rules described above.

Reference is now made to Fig. 5, which shows a graphical representation of the chart of Fig. 4. Within the compartments that proliferation occurs (SC and CFU-Meg), the number of proliferating cells increases from the first to the last age-section. In contrast, the cell number in the compartments that have no proliferating ability remains constant (MKB, MK128, PL), or decreases when cells that have undergone additional endomitosis leave the compartment for the next one (MK16, MK32, MK64).

Reference is now made to Fig. 6, which is an illustration of another representation of the model, based on the time courses of different compartments. The rows in the chart represent cell compartments and the columns represent time of simulation course. At every time-step of the simulation (one hour of "patient's life"), the number of cells in all age-sections is summarized for each compartment and the next column in time-course chart (Fig. 6) is filled. Thus, every cell in the chart represents the total number of cells in a given compartment at a given time point.

There is an additional row in the time-course chart that relates to the TPO concentration in the blood. TPO concentration is written down every time-step concurrently with the cell numbers.

Reference is now made to Fig. 7, which is a graphical representation of the chart of Fig. 6, and is the most useful model output **[why? Describe graph and how it is used]**.

The implementation of the described model results in a computer simulator that describes the changes that occur in the human thrombopoietic system (platelet counts, bone marrow precursor numbers, and TPO concentration) over several years. The resolution of the simulator output is one hour.

Time units and periods that we will speak about relate to the simulated patient's life, not to the running time of the program.

IV. PARAMETER-SPECIFIC ADAPTATION OF MODEL

This model may be fit to patients with diverse blood and bone marrow parameters. People differ in their baseline platelet counts and numbers of bone marrow precursors, in the cells' transit times and amplification rates,

rates of platelet release by megakaryocytes, fractions that each megakaryocyte ploidy class donate for additional endocytosis, and in the time needed for endomitosis. Furthermore, the rate of TPO production, receptor- and non-receptor-mediated TPO clearance, the threshold of TPO effect on

5   SC compartment 30, and the sensitivity of different cell parameters to TPO also differ from one person to the next.

To obtain an ideal fitness of the model to each patient, the patient-related parameters should be given individually for each patient. However, practically, it would be extremely difficult to predetermine many of these

10   parameters for every patient. Therefore, certain average parameters have been calculated based on published data, and are shown in Table 1 below. These averaged parameters are used as a framework into which known individual characteristics are included. Thus, before a particular simulation is begun, relevant known information about the individual may be included,

15   sometimes replacing certain parameters of the model.

TABLE

Feature / Compartment	Baseline number (x 10^3/kg)	Normal amplification rate (increase per hour)	Normal transit time (hrs)	Normal cell flow* (hour^{-1})	Rate of platelet release (hour^{-1} x megakaryocyte^{-1})	Time needed for additional endomitosis (hrs)
SC	478	1.029	24	0.342	----	----
CFU-Meg	1250	1.0255	60	1	----	----
MKB	5105	----	132	1	----	----
MK16	4080	----	120	0.26	10.2	48
MK32	1250	----	120	0.016	20.4	48
MK64	15	----	120	0.4	40.8	48
MK128	7.5	----	120	----	81.6	----
PL	15 050 000	----	240	----	----	----

TPO-related parameters	Rate of production	Non-receptor-mediated clearance	Receptor-Mediated clearance	Threshold for the effect on SC		
	7 pg/ml/hr	3 % /hr	4.776×10^{-10} pg/ml/receptor/hour	2500 pg/ml		

Steepness of the TPO sensitivity curve of	SC amplifica tion rate	CFU-Meg amplification rate	CFU-Meg transit time	MKB transit time	Fraction of MK16 undergoing additional	Fraction of MK32 undergoing additional	Fraction of MK64 undergoing additional

28

different parameters (St)					endomitosis	endomitosis	endomitosis
	4***	30	100	7	3	3	3

* - fraction of mature cells of a given compartment that goes to the next compartment
** - Sensitivity of the intrinsic TPO-independent mechanism that determines SC amplification rate (S) is 0.2.
*** - the logarithm base is 10, not e, like in others

5

Usually, the known patient-related data are not parameters in the form defined by our model, but rather measurements obtained in the clinic (e.g., day and value of post-chemotherapy thrombocytopenia nadir, day and value

10   of platelet peak after TPO administration, change in megakaryocyte modal ploidy following some perturbation, etc.). In these cases, the available data is converted into a model-compatible format.

Sometimes, the only available patient-related data is the graphic representation of the patient's platelet course following some perturbation

15   (e.g., cell-suppressive therapy or TPO administration). The data may also be a picture of the platelet course without any external disturbance (e.g., cyclic thrombocytopenia). In these cases the model parameters are changed by trial-and-error until a good compliance of the model graphic output and the patient's graphs is achieved. It should be noted, however, that even in the

20   case of trial and error, the choices of parameter sets are not random but rather are also based on some analysis **[for example?]**.

Specifically, the following tools are available for providing maximum flexibility:

1) The user can set the baseline values and all other known patient-

25   specific thrombopoietic parameters before starting the simulation.

2) The user (e.g., physician) can determine how long of a time period to simulate, from 12 hours up to several years.

29

3) The user can determine the frequency of showing the course of a patient counts up to the moment. The frequency can change from as much as every 12 hours to once during the overall period of simulation.

4) The user can determine the resolution of the output graph, from the hourly representation of the patient's state down to any other resolution. **[What does this mean? Can it be resolved at units of less than an hour? If so, how?]**

5) The user can choose to view the graphical representation of the age distribution through the compartments at any moment of the simulation.

6) The user can imitate a cell-suppressive therapy at any moment while running the simulation by reducing one or several of the compartments by any value.

7) The user can simulate exogenous TPO administration at any moment while running the simulation by controlling dose height, number of dosings or frequency of dosings.

The simulation tool has been carefully tested with respect to the published experimental results, and has proved to be well calibrated for average human data. Parameters may be modified relatively quickly for efficient use of the system. The following model parameters are important for individualized adjustment of the model:

- baseline number of: SC, CFU-Meg, MKB, MK16, MK32, platelets.
- amplification rate of: SC, CFU-Meg.
- transit time of: MKB, MK16, MK32, MK64.

30

- fraction undergoing additional endomitosis in: MK16, MK32, MK64.

- rate of platelet release of: MK16, MK32, MK64, MK128.

- Time needed for additional endomitosis.

- Rate of endogenous TPO production.

- Ratio of receptor- and non-receptor-mediated TPO clearance.

- Steepness of the sensitivity curve of: CFU-Meg amplification rate; MKB transit time; MK16, MK32, and MK64 fraction undergoing additional endomitosis.

[Question: which of these parameters can actually be measured and input into the program? All? Are there other parameters too such as age, weight, medical history, etc.? I think we need to distinguish between types of parameters.]

Reference is now made to Figs. 8A, 8B, 9A and 9B, which show a comparison between experimentally obtained data and the simulated model. Experimentally obtained *in vivo* platelet counts following TPO administration are shown in Fig. 8A **[is this with chemotherapy too?]**, and chemotherapy without TPO is shown in Fig. 9A. Figs. 8B and 9B show simulations of the same. By using a TPO schedule designed by the described model, one can obtain platelet profiles that are similar to those obtained clinically (Fig. 8B) or even more effective (Fig. 9B). In this case, these results are achieved by administering a pre-calculated TPO protocol whose total dose amounts to 25% of the original total dose. **explain the point of this better**

The complete model simulates cell and platelet counts in the steady state, as well as after perturbations to the hematopoietic system, e.g., cell-suppressive therapy, recombinant thrombopoietin administration, etc. It is

possible to simulate any protocol of drug administration and any hematological state of a patient, regarding his/her platelet count and number of bone marrow megakaryocytes and their precursors. The model can be adapted to many categories of patients, or healthy platelet donors. It can also

5   be modified to fit species other than human. By providing specific parameters one can adjust the model so as to yield particular predictions about the thrombopoietic profile of an individual patient.   Platelet disorders, such as cyclic thrombocytopenia, may also be simulated.

EXAMPLE 2: Neutrophil Bone Marrow and Peripheral Blood Compartment under the Effects of Growth-Factors and Treatment with Granulocyte Colony Stimulating Factor (G-CSF)

The neutrophil lineage originates in pluripotent stem cells that proliferate and become committed to the neutrophil lineage. These cells then undergo gradual maturation accompanied with proliferation through the three morphologically distinguishable mitotic compartments: Myeloblasts, promyelocytes and myelocytes. The myelocytes then mature and lose their capacity to proliferate, and thus enter the post mitotic compartment. In the post-mitotic compartment the cells continue their gradual maturation, which is not accompanied with proliferation through the three morphologically distinguishable sub-compartments: Metamyelocyte, band and segmented-neutrophils. Cells exit the various sub-compartments in the post-mitotic compartment and enter the blood as neutrophils. They then migrate from the blood to the tissues.

The Granulocyte-Colony Stimulating Factor (G-CSF) effects an increase in blood neutrophil levels primarily by increasing production in the mitotic compartment and shortening the transit time of the post-mitotic compartment.

Thus, the first compartment of the mitotic pool (myeloblast) receives an inflow of cells from stem-cell precursors. Inflow for each of the other compartments is from outflow of the previous one, subject to multiplication factors due to cell replication in the mitotic stages.

Models regarding granulopoiesis in normal humans and in humans with pathologies of the bone marrow were suggested previously in order to give a coherent description of the kinetics of granulocytes from experimental data (Cartwright – 1964, Mary – 1978, Rubinow – 1974). In recent years

5 Schmitz et al. developed a kinetic simulation model for the effects of G-CSF on granulopoiesis (Schmitz – 1993), and used it for the analysis of administration of G-CSF to patients suffering from cyclic neutropenia (Schmitz – 1995). However, the data Schmitz rests upon for his model has been more accurately assessed in recent years by Price et al. (1998) and Chatta et al.

10 (1996). Actual empirical data regarding compartment sizes and their transit times was not incorporated into their model despite the importance of these data (Dancey et al. 1976).

34

I. MODEL OF NEUTROPHIL LINEAGE AND EFFECTS OF G-CSF

A. G-CSF

The effects of G-CSF on the neutrophil lineage are relayed in the model in three stages. The first is the administered amount of cytokine given at time t, which is marked: G^t_{adm}

The G_{adm} vector serves as the control variable for optimization of G-CSF administration.

The second stage represents the pharmacokinetic behavior of G-CSF in circulation. It incorporates, for instance, the half-life of G-CSF, and could in the future be modified to express more of the effects of time on G-CSF activity. This level is marked G^t_{blood}.

G-CSF is eliminated from the blood in a Poissonic manner according to the following equation, as stated by Stute N, Furman WL, Schell M and Evans WE in "Pharmocokinetics of recombinant human granulocyte-macrophage colony stimulating factor in children after intravenous and subcutaneous administration"" Journal of Pharmaceutical Science, 84(7): 824-828, 1995:

$$G^{t+1}_{blood} = G^t_{blood} \left(1 - \frac{\ln 2}{\tilde{t}_{\frac{1}{2}}}\right) + G^{t+1}_{adm}$$

(14)

where $\tilde{t}_{\frac{1}{2}}$ is the half-life of G-CSF in the blood, and $G^1_{blood} = G^1_{adm}$

Recent data by Terashi K, Oka M, Ohdo S, Furudubo T, Ideda C, Fukuda M, Soda H, Higuchi S and Kohno S, in "Close association between clearance of recombinant human granulocyte colony stimulating factor (G-CSF) and G-CSF receptor on neutrophils in cancer patients", Antimicrobial

35

Agents and Chemotherapy, 43(1): 21-24, 1999, points to the dependence of the half-life of G-CSF on neutrophil counts. In the absence of exact kinetics of G-CSF effects on the neutrophil lineage, the half-life is considered as a constant, though this could be modified should more exact information

5   emerge.

Only exogenously produced G-CSF is considered to affect the kinetic parameters, and endogenously produced G-CSF levels and effects are set to zero. If more empirical data regarding the production of endogenous G-CSF is made available, it could be incorporated into the equation as well.

10   The third and final stage models the pharmacodynamic effects of G-CSF on the kinetic parameters. As will be elaborated subsequently, the dependence of the various kinetic parameters of the neutrophil lineage on the level of G-CSF in the blood is assumed to be through either non-decreasing concave or non-increasing convex functions. This reproduces the effects of

15   saturation that are seen in clinical studies on the effects of G-CSF, such as the study by Duhrsen U, Villeval JL, Boyd J Kannourakis G, Morstyn G and Metcalf D in "Effects of recombinant human granulocyte colony-stimulating factor on hematopoietic progenitor cells in cancer patients", Blood, 72(6): 2074-2081, 1988. That is, addition of G-CSF carries a lesser effect when its

20   level in circulation is already high.

B. Biological Model

Mitotic Compartment

Long-term effects of G-CSF administration take place in the mitotic compartment. Although the major contributor to heightened blood

neutrophil counts in the short term is the post mitotic compartment's shortening of transit time due to G-CSF administration, this high level cannot be maintained over the long term without increased production in the mitotic compartment.

5   The mitotic compartment is divided into subcompartments. The k*th* subcompartment contains all cells of chronological age between k-1 and k hours, relative to the time of entry into the mitotic compartment. The number of cells in subcompartment k at time t is marked as m_k^t.

$$k \in \{1..\tau\}$$

10

$$m_1^t = \ell_1^t (G_{blood}^t)$$

(15)

where τ is the transit time of the entire mitotic compartment, and is assumed to be the same and constant for all cells entering the mitotic compartment, and l_1 is a vector reflecting the flow of newly committed cells into the mitotic

15   compartment. The biological grounds for this definition is the existence of a myeloid stem cell reservoir, which is known to supply new committed cells to the mitotic compartment. However, the reservoir's actual kinetics are not very well explored empirically. We therefore fix l_1 to levels such that the overall

20   size of the mitotic compartment as well as the kinetics of the neutrophils in circulation would match those obtained empirically.

Any new biological data that emerges may help define the kinetics more accurately within the framework of this model, although results of this model indicate that the assumption of a constant rate of stem cells flowing

into the mitotic compartment in the absence of G-CSF is plausible. For every $n \in \{1..\tau\}$, and for every t, amplification occurs at the exit from m_n^t, according to Equation 15 as follows:

$$m_{n+1}^{t+1} = m_n^t \cdot \alpha_n(G_{blood}^t)$$

(16)

where:

α_n is a non-decreasing concave function of G-CSF levels in the blood, which determines the factor of amplification in the hourly subcompartment n. If, for instance, no amplification occurs at subcompartment n_0 at time **X?** then

$$\alpha_{n_0} = 1$$

$$\forall n, G_{blood}^t \quad 1 \le \alpha_n(G_{blood}^t) \le 2$$

(17) The size of the morphological sub-compartments in the mitotic compartment at time t is determined as:

(18) Where n_0 is the first hourly sub-compartment of a morphological sub-compartment and n_1 is its last hourly sub-compartment. The division into the morphological sub-compartments is used only for fine-tuning of the kinetic parameters with the use of experimental data.

The mitotic compartment was modeled with an intention to facilitate the specific cell-cycle cytotoxic effects of chemotherapy. Therefore, cohorts of one hour are modeled as undergoing a process of maturation and amplification culminating in their entry into the post-mitotic as described below. Effects of chemotherapy may be incorporated into the model by mapping the various cell-cycle phases (G1, S, G2, M) to the hourly cohorts

modeled and formulating a function of the cytotoxic effects of chemotherapy on these phases.

The experimental literature shows wide agreement regarding the steady state normal amounts of circulating neutrohpils, size of the post-mitotic compartment and the three morphologically distinct sub-compartments of the mitotic compartment, and post-mitotic transit time and amplification rates in the mitotic sub-compartments (see, for example, Dancey JT, Deubelbeiss KA, Harker LA and Finch CA, in "Neutrophil kinetics" in Man. Journal of Clinical Investigation, 58(3): 705-715, 1976; Price TH, Chatta GS and Dale DC, "Effect of recombinant granulocytee colony-stimulating factor on neutrophil kinetics in normal young and elderly humans", Blood 88(1): 335-340, 1996; and Dresch Mary in "Growth fraction of myelocytes in normal human granulopoiesis", Cell Tissue Kinetics 19: 11-22, 1986). To determine other relevant kinetic parameters, which were either not available in the literature or were given a wide range by experimentalists, steady state kinetics was assumed and an iterative process was employed. These parameters include the inflow of stem cells to the myeloblast compartment and the transit times of the mitotic sub-compartments.

The half life of blood neutrophils and the steady state number of neutrophils were taken as 7.6h and 0.4×10^9 cells/kg body weight, respectively (Dancey et al., 1976). Similarly, the same calculation may be made for each patient that is to be modeled. This would allow the dynamics of every patient to be described by the simulation. The average size of the post-mitotic compartment (5.84×10^9 cells/kg body weight – Dancey, 1976) and the transit time of the compartment (160h – Dancey, 1976; Mary, 1986; Price, 1996) are

39

compatible with the size and half-life of the circulating neutrophil compartment reported by Dancey, thus supporting the steady state analysis.

In order to determine the amount of cells in the hourly sub-compartments in the mitotic compartment, all compartments in the lineage were modeled using a steady state assumption. The number of cells exiting the circulating neutrophil pool equals the number of cells exiting the post mitotic compartment, which in turn equals the hourly production of cells in the mitotic compartment. Thus, the number of cells in the last hourly cohort of the mitotic compartment can be determined from the neutrophil decay rate, which is available in the literature. However, this calculation is based on assumptions that there is no apoptosis in the post-mitotic compartment. Direct experimental data by Thiele J, Zirbes TK, Lorenzen J, Kvasnicka HM, Scholz S, Erdmann A, Flucke U, Diehl V and Fischer R, in "Hematopoietic turnover index in reactive and neoplastic bone marrow lesions: Quantification by apoptosis and PCNA labeling," Annals of Hematology 75(1-2): 33-39, 1997, suggests that apoptosis is not a significant phenomenon in normal human bone marrow. The size calculated for the mitotic compartment is close to that experimentally obtained by Dancey and Price, thus supporting the notion that apoptosis is not a significant kinetic factor in the lineage. Values for the production of cells in the mitotic compartment can later be modified in light of new evidence.

Regarding the transit time of the mitotic compartment there is little agreement in the literature, with a range of 90-160 hours given by most experimentalists (see Dresch Mary in "Growth fraction of myelocytes in normal hman granulopoiesis," Cell Tissue Kinetics 19: 11-22, 1986). In order

40

to determine the transit times of the mitotic morphological sub-compartments, as in Equation **18**, the following constraints were considered:

1. The sizes of the theoretically obtained morphological sub-compartments must fit those reported experimentally in normal human hematopoiesis (Dancey, 1976) and under the effects of G-CSF (Price, 1996);

2. At least 24 hours, the typical cell cycle, must separate amplification points;

3. The size of the last hourly sub-compartment must equal the hourly production of the mitotic compartment (calculated with the aforementioned iterative process assuming steady state kinetics);

4. Amplification inside the compartment is set at the levels determined by Mary 1984; and

5. The total transit time of the mitotic compartment must be within the 90-160 hour range.

By using the values shown in Table x, an excellent fit was obtained within the above-mentioned constraints.

It should be noted that when other alternatives with shorter transit times were attempted, results could not be obtained that agreed with the literature regarding the size of the mitotic pool or its production. **Furthermore, a fit between our simulation model's results regarding PMN counts in peripheral blood with empirical data could not be achieved without speculating extensively on the nature of G-CSF effects**

on non-committed stem cells (data not provided). It should be noted, that little empirical quantitative data is available regarding stem cells.

The effects of G-CSF on this compartment are modeled as an increase in the rate of cells entering the myeloblasts from the uncommitted stem cell pool, increases in the rates of mitosis, and introduction of new points of amplification as shown in Equation **15, 16**. Since little data is available regarding the increases in amplification due to G-CSF, an initial assumption was made that amplification reaches full potential at points that under normal conditions undergo an amplification of below a factor of 2. Additionally, it was assumed that the transit time in all mitotic sub-compartments and the typical cell cycle duration are not affected by G-CSF, based on lack of evidence to the contrary.

Reference is now made to Figs. X and y, which show a comparison of neutrophil production according to the described model and experimental data in the literature. Increased neutrophil production is in accordance with the neutrophil counts reported by Price et al. In addition, these increases are in accordance with Price's data about neutrophil bone marrow pool sizes.

Reproduction of the effect of G-CSF on neutrophil counts and the mitotic compartment sizes beyond day 5 of administration was accomplished by assuming an increase (15% with the highest dose of G-CSF) in the rate of cells entering the myeloblast compartment. Alternatively, G-CSF may change the behavior of the myeloblast compartment such that some of the cells there undergo self-renewal instead of moving on to the promyelocyte compartment. However, no empirical data to support this is available. The model can be modified in light of new experimental data in the future.

42

Post-mitotic compartment

The post mitotic compartment is relatively insensitive to cytotoxic chemotherapy. Therefore, it is biologically acceptable and computationally sensible to model this compartment as a single pool of cells, such that the last hourly cohort of the mitotic compartment enters the compartment, and a proportion of the cells within the compartment enter the neutrophil pool every hour.

The post mitotic compartment at time t is a single quantity of cells p^t, such that:

$$p^{t+1} = l_3(G_{blood}^t) \cdot p^t + m_\tau^t$$

(19)

where l_3 is a convex, non-increasing function of G-CSF levels in the blood, which takes values in the range of [0-1]. This definition entails $p^t > 0$.

G-CSF affects the post-mitotic compartment by shortening its transit time (i. e. decreasing l_3). Price notes that the number of cells in the post mitotic compartment is not significantly changed following administration of G-CSF. This determination is based on counts made on day 5 after G-CSF administration. Thus, it can be safely assumed that any increased production of the mitotic compartment flowing into the post mitotic compartment is translated over the long-term to an increase in the flow of cells from the post mitotic compartment to the neutrophil pool. This increased flow is compensated by increased production in the mitotic compartment only at a

43

later stage. Therefore, an upper limit to the number of cells in the post mitotic compartment was set, which is at the values given as steady state counts (Π).

In brief, the effects of G-CSF on the neutrophil lineage are modeled during the first few days primarily as a decrease in the counts of the post-mitotic compartment, which is then compensated by an increased production in the mitotic pool. This compensation sustains the increase in neutrophil counts in peripheral blood.

Reference is now made to Fig. 11, which is a graphical illustration of a simulation of the model. Though no empirical data is available on this point, simulations of the model predict that the number of cells in the post-mitotic compartment decreases substantially during the first two days of G-CSF administration, and then replenishes, so that on the sixth day the counts return almost to their normal levels. This replenishment lags behind that of Price et al report by a few hours. We can thus formulate a **testable hypothesis**, i.e., whether using the same G-CSF protocol Price et al used, there is indeed a nadir on day 3 of the treatment.

Compartment	Day 0 (no G-CSF) (x10^9 cells/ kg. Body weight)	Day 15 of G-CSF treatment (x10^9 cells/ kg. body weight)	Relative increase in compartment size due to G-CSF
Myeloblasts	0.140	0.153	1.09
Promyelocytes	0.582	0.898	1.54
Myelocytes	1.373	3.564	2.60
Mitotic Total =	**2.10**	**4.615**	**2.20**
Circulating neutrophils	0.4	2.35	5.88

Table 1. Simulated kinetics after 15 days of subcutaneous administration of 300μg G-CSF/kg weight. Day 0 values are the mean values Dancey et al (1976) use.

We shall mark as o^t the outflow from the post mitotic compartment:

$t+1$

The number of neutrophils in the circulating blood compartment at time t is marked n^t and is modeled as a single quantity of cells, such that:

$$n^{t+1} = o^t + n^t (1 - \frac{\ln 2}{t_{\frac{1}{2}}})$$

(21)

where $t_{\frac{1}{2}}$ is the half-life of neutrophils in the blood, as defined in the biological literature, and is assumed to be constant regardless of G-CSF levels (Lord 1989), though this could be easily modified. The kinetics of neutrophils in the tissues are not modeled in this work.

Neutrophils and G-CSF in the Circulating Blood

The elimination of neutrophils from peripheral blood follows a Poisson distribution, and can therefore be described as an exponential function (Cartwright, 1964). Therefore the rate of cells leaving this compartment is based on half-life determinations available in the literature. Since no direct cytotoxic effects of chemotherapy have been described for this compartment it is also modeled as a single pool of cells.

At the normal healthy level we have the following relationship:

$$G^t_{blood} = 0, p^t = \Pi, m^t_\tau$$

$$\frac{\Pi}{T} = m^t_\tau = o^t = \frac{n^t}{t_{\frac{1}{2}}} \times \ln 2$$

which reflects the stability of the steady state.

The kinetics of G-CSF is also modeled as an exponential distribution with a half-life of 3.5 hours (Stute, 1992) **(Eq. 14)**.

The effects of G-CSF on the kinetics of the neutrophil lineage appear not to be a linear function of G-CSF administration levels. Since data provided in the literature (Chatta 1994) only refers to two doses (30 and 300μgram/kg body weight) we can only speculate on the effects of other levels of G-CSF. After trial and error analysis, it was found that assuming that the effects of the 300-μgram dose are the maximal, at the 30-μgram its effects are about 30% of the maximum.

Reference is now made to Figs. 12A and 12B, which are graphical illustrations of the effects of G-CSF at the two doses. The effects as a function of G-CSF level are connected piece-wise linearly. This way, the neutrophil levels observed clinically under both the 300 and the 30-μgram protocols are obtained.

II. LINEAR IMPLEMENTATION OF THE MODEL

This model will later be incorporated into an optimization scheme that will have as its objective function both the aims of minimizing G-CSF administration and returning the neutrophil lineage to its normal levels.

Although the above-outlined model may be implemented in any number of optimization methods, linear programming was chosen because of its inherent advantages compared with other techniques, i.e. its ability to provide an optimal solution using partially analytical methods, and therefore

4/6

being more computationally tractable (Gill 1991). On the other hand, implementation of this model in linear programming carries with it the disadvantage that certain computations must be approximated linearly since they cannot be performed directly using linear methods. Thus, we shall

5   compare the 'closeness' of the solution obtained through linear programming will be compared with that obtained through another, non-linear method of optimization.

The significant parts of the model that must be modified due to the linear programming implementation are the sections in which multiplication of

$$\{(x_{\min}, y_{\min}, x_{\min} \cdot y_{\min}), (x_{\min}, y_{\max}, x_{\min} \cdot y_{\max}), (x_{\max}, y_{\min}, x_{\max} \cdot y_{\min}), (x_{\max}, y_{\max}, x_{\max} \cdot y_{\max})\}$$

10   two variables is defined, since this operator is not itself linear. Therefore, multiplication is defined as an approximated value constrained within piecewise linear constraints that most closely bound the product within a four-faced polyhedron in 3-dimensional space whose vertices are

15   Where x_{min}, x_{max}, y_{min}, y_{max} are the constant biologically defined minima and maxima of x and y.

$$M(x, y) \begin{cases} \geq y_{\min} x + x_{\min} y - x_{\min} y_{\min} \\ \geq y_{\max} x + x_{\max} y - x_{\max} y_{\max} \\ \leq y_{\min} x + x_{\max} y - x_{\max} y_{\min} \\ \leq y_{\max} x + x_{\min} y - x_{\min} y_{\max} \end{cases}$$

(22)

Multiplication may also be approximated with variations on the linear least squares method, by finding one plane that's closest to the four vertices

20   defined.

47

The other functions that need to be defined linearly are those concerning the pharmacodynamics of G-CSF. Due to the nature of these functions (either non-increasing convex or non-decreasing concave), these effects are implemented as piece-wise linear functions whose breakpoints are

5 the doses for which actual experimental data is available (Chatta 1994). Note that the effects of G-CSF on each of the kinetic parameters have not been determined in a detailed manner by experimentalists. Rather its effects over a few dose levels on the neutrophil blood counts and the size of the morphologically different mitotic compartments and the post mitotic

10 compartment have been determined. From these data, the effects of G-CSF on the actual kinetic parameters (probability of mitosis, transit time and inflow of cells into the myeloblast compartment from stem cell progenitors) has been reconstructed at the dose levels available in the literature. These points are then connected linearly to obtain piecewise linear functions relating G-CSF

15 levels to their effect on those parameters. Further experimental data in the future could be used to produce more accurate functions.

At the amplification points within the mitotic compartment, the linearly approximated multiplication operator **(Eq 22)** is used instead of the product defined in **Eq. 16**.

20 At points where no amplification occurs the quantity from one compartment is simply transferred to the next according to the following Equation:

$$m_{n+1}^{t+1} = m_n^t$$

$$m_n^0$$

Values are set according to the steady state values of the mitotic compartment, or are depleted according to the kill function of the chemotherapy.

5   The flow out of the post mitotic compartment **(Eq. 20)** is similarly defined as a linear approximation of a product.

3. Formulation of the Model as an Optimization Problem for Linear Programming

The simulation spans a finite number of discrete time steps denoted by *T*.

10   We define as the control variable the vector that represents G-CSF administration at every given hour t, $G_{adm}^t, t \in \{1..T\}$

The objective function is defined as maximization of the following expression:

$$\sum_{t=1}^{T} (\beta^t \cdot p^t - G_{adm}^t)$$

(Eq. 24)

15   where p^t is the number of cells in the post mitotic compartment at time *t*, and • is a scalar weighting coefficient. The logic for formulating the objective function this way is that the ability to maintain the post mitotic compartment's steady state size for a prolonged period of time is sufficient for rehabilitation of the neutrophil lineage as a whole. Also, our goal is to minimize the total

20   administered quantity of G-CSF. • is introduced to allow us to factor in both these goals in one objective. Also, this would allow a different weight to be given for certain times, e.g. were it determined (by clinicians) that the later states of the post-mitotic compartment should be weighted more than the first

49

ones. Obviously this is only one of the possible formulations of the objective function as defined in the previous section.

The pharmacokinetics and pharmacodynamics of G-CSF that were defined generally in the mathematical model are defined piecewise linearly. Some of the considerations that we put into formulating these functions were based directly on experimental evidence (elaborated in the main body of text). We note however, that actual experimental data regarding the direct effects of G-CSF on the kinetic parameters in which this model is interested is rather scant. Therefore, some formulations were conducted through partly analytic and partly trial-and-error methods.

The formulation of the model in piecewise linear terms will allow use of this model as a clinical tool in three ways. First, the model will determine the effectiveness of various protocols suggested by clinicians prior to their actual use on human patients. Second, the model allows computation of the optimal protocol in a given situation of neutrophil counts, so that the neutropenic period following chemotherapy is either shortened or completely avoided at a minimal cost and exposure to G-CSF. Third, the model serves as a constituent in a broader framework of clinical tools that will compute the most optimal treatment plan for chemotherapy and growth factors. These uses should help clinicians administer more rational treatment to their patients minimizing both suffering and medical costs.

Amplification at the exit	Mean transit time (hours)	Size (10^6 cells/kg weight)	Compartment
2^+	24^-	0.139^*	Myeloblasts
2^+	48^-	0.558^*	Promyelocytes
1.5^+	48^-	1.4^*	Myelocytes
1	160^*	5.84^*	Post mitotic
0	10.96^*	0.4^*	Neutrophils

Table 1. Kinetics under steady state conditions in healthy humans.
*Dancey, 1976.
+Dresch, 1986.
-Calculated based on the steady state assumption as elaborated in the main text.

EXAMPLE 3: Cancer and Treatment with Cytotoxic Drug Delivery

Introduction

Cancer is the second leading cause of mortality in the US, resulting in approximately 550,000 deaths a year. There has been a significant overall rise in cancer cases in recent years, attributable to the aging of the population. Another contributing factor to the rise in the verifiable number of cases is the wider use of screening tests, such as mammography and elevated levels of prostate specific antigen (PSA) in the blood.

Neither better detection nor the natural phenomenon of aging, however, can entirely explain the increase in new cases of tumors. Meanwhile, other cancers, like brain tumors and non-Hodgkin's lymphoma, are becoming more common. Their increase could reflect changes in exposures to as yet unidentified carcinogens. Current trends suggest that cancer may overtake heart disease as the nation's no. 1 killer in the foreseeable future. As gene therapy still faces significant hurdles before it becomes an established therapeutic strategy, present control of cancer depends entirely on chemotherapeutic methods.

Chemotherapy is treatment with drugs to destroy cancer cells. There are more than 50 drugs that are now used to delay or stop the growth of cancer. More than a dozen cancers that formerly were fatal are now treatable, prolonging patients' lives with chemotherapy.

Treatment is performed using agents that are widely non-cancer-specific, killing cells that have a high proliferation rate. Therefore, in addition to the malignant cells, most chemotherapeutic agents also cause severe side-effects because of the damage inflicted on normal body cells. Many patients

develop severe nausea and vomiting, become very tired, and lose their hair temporarily. Special drugs are given to alleviate some of these symptoms, particularly the nausea and vomiting. Chemotherapeutic drugs are usually given in combination with one another or in a particular sequence for a relatively

5   short time.

Chemotherapy is a problem involving many interactive nonlinear processes which operate on different organizational levels of the biological system. It usually involves genomic dynamics, namely, point mutations, gene amplification or other changes on the genomic level, which may result in

10   increasing virulence of the neoplasia, or in the emergence of drug resistance. Chemotherapy may affect many events on the cellular level, such as cell-cycle arrest at different checkpoints, cell transition in and out of the proliferation cycle, etc. Chemotherapy may also interfere with the function of entire organs, most notably, with bone marrow blood production. In recent years molecular biology

15   and genetics has made an important step forward in documenting many of these processes. Yet, for assessing the contribution of specific molecular elements to the great variety of disease profiles, experimental biology must be provided with tools that allow a formal and systematic analysis of the intricate interaction between the genomic, cellular and cell population processes in the

20   host and in the disease agent. This system is so complex that there is no intuitive way to know how small changes in the drug protocol will affect prognosis. But in spite of this intricacy, attempts to improve chemotherapy have been carried out by "trial and error" alone, with no formal theory underlying the application of specific drug schedules. Such an approach "is apt to result in no

improvement, only discouragement and little useful information for future planning" (Skipper, 1986).

The treatment of cancer by cytotoxic drug (or drug combination) delivery is addressed. In this model, two generic types of cells are considered: host cells and target cells. Target cells are, in fact, the tumor. Both types of cells may be damaged while exposed to chemotherapy. The aim is to obtain the most suitable treatment protocol according to specified conditions and limitations. It is assumed that the cell dynamics are deterministic and known, and that both types of cells are sensitive to chemotherapeutic agents in certain known period of the cell-cycle phases. If a cell is exposed to chemotherapy during part of its critical phase, there is a chance that it will be eliminated, blocked or affected in any other known way. The description of the dynamics of the delivered drugs is assumed to be known as well.

In order to achieve the goal optimization process is applied to the model. The optimization module uses the model predictions in order to search for the suitable solution to posted optimization problem. Precise defining of optimization objectives as well as the relevant parameters adjustment is done according to the settings defined by user/operator for every special case. The method can be applied in general cases as well as in specific ones.

2. Model of Biological System

The basic layer of the model incorporates a description of age distribution of cycling cells and number of resting (quiescent) cells. The term

54

"age of the cell" here refers to chronological age starting from the conventional beginning point of mitotic cycle.

Reference is now made to Fig. 13, which is a schematic illustration of the tumor cell cycle layer. The whole cycle is divided into 4 compartments, or stages (G_1, S, G_2 and M). Each compartment is divided into equal subcompartments, where i^{th} subcompartment in each stage represents cells of age i in the particular stage (i.e. they have spent i time-steps in this stage). The quiescent stage is denoted G_0. The cell cycle follows a direction as shown by arrows (#). Thus, cells enter each stage starting with the first subcompartment, denoted G_1.

The model can be described mathematically as follows: Let T_k denote the maximum duration of kth stage in the cycle. Let $\bullet$ t denote the time resolution of the model in discrete time steps. $X_k^i(t)$ is a function, which represents the number of cells in stage k in the Ith sub-compartment, at time t to $t+\bullet t$. Both time and age are measured in the same unit, in this case, hours. Let $Q(t)$ represent the number of resting cells at time t to $t+\bullet t$. $Trans(k,i,t)$ represents the probability that a cell of age i in the stage k will move to the next ($k+1$) compartment. Cells entering the new stage always start from the first subcompartment, i.e. from $i=1$. This probability may change with time, representing the influence of conditions on cycle length distribution.

By definition, the cell cannot remain more than T_k timesteps in the kth compartment, as described in the following equation.

$$\forall\ k\ :\ Trans\ (k, T_k) = 1$$

The restriction point (R-point) represents a cell's commitment to complete the mitotic cycle. Let T_R denote the age at which the cell passes

55

through the restriction point in G1. Only cells in G_1 with $I < T_R$ can the cycle (in the absence of a drug).

The total number of proliferating cells P(t) can be calculated as follows:

5

$$P(t) = \sum_{k=G1,S,G2,M} \left(\sum_{i=1}^{T_k} x_k^i(t) \right)$$

In every time interval, quiescent cells may return to the proliferation pool. Alternatively, proliferating cells may change their state to become

10 quiescent if and only if they are in the G1 stage and at age i, where $T_R \bullet i > 0$. To describe this process we introduce the function $G_{1 \bullet 0}(i,t)$ which describes the number of G1 cells in age i which become quiescent during time interval $[t, t+ \bullet t]$. This function may receive negative values, accounting for cells that return from resting to proliferation.

15 As we assume that the exit to quiescence can occur only prior to the R-point (even in cancer cells), and that a resting cell that returns to proliferation enters the cycle at T_0, it can be stated:

$$\forall i > T_R, \forall t : G_{1 \to 0}(i,t) = 0$$

20 It must be noted that this function is not dependent on i and t solely. Its value is determined according to current cell distribution and all the general parameters that characterize the described cells group. The same should be said about the values of *Trans* vector that can change during the history of given population.

The model traces the development of described group of cancer cells using given parameters, by calculating the number of cells in each and every subcompartment according to the following stepwise equations:

$$
x_k^i(t) = \begin{cases}
x_k^{i-1}(t-1)\cdot[1-Trans(k,i-1,t-1)], & 1 < i \le T_k \\
\sum_{j=1}^{T_{G1}} [x_{k-1}^j(t-1)\cdot Trans(k-1,j,t-1)]\cdot[1-G_{1,0}(i-1,t-1)], & i=1
\end{cases}
$$

for $k=G_2, M$, $k-1$ returns the previous stage (e.g. $G_2-1=S$).

These equations make it possible to calculate the number of cells in each subcompartment at every time interval $[t, \bullet \, t]$ starting from initial distribution (e.g. at time $t=0$). Since in this model cell ages are measured in absolute time units, these measurements refer to the chronological age of the cell, and not the biological age, whose units are relative to a maturation rate that differs from cell to cell. Consequently, in this model no cell can remain in the same age subcompartment after every time step. On the other hand, a fraction of the cells that leaves any subcompartment may be transferred to the first subcompartment of the next stage, according to probability vector

Trans(k,i,t). This vector provides the ability to account for variability of cycle lengths while retaining a deterministic approach.

The behavior of the cell population in this model is completely controlled by two components: *Trans* vector, and *G1→G0* function. These two functions determine uniquely the outcome of every single time step, and, consequently the result over long periods. Thus, they are referred to as "*control functions*". The values of these functions may be dependent not only on time and age of cells, but also on the current population state (or, generally, on the whole history of the population) as well as on the environment associated with a given cell group. However, those parameters are similar for all the cells in the group, implying that the model presented here is suitable for describing highly homogenous group of cells. Therefore, the basic layer of the model should give a realistic description for a uniform group of cancer cells for which environmental conditions and relevant biological properties are defined, in a way that will allow the construction of the control functions for the group.

2.2. The General Tumor Model

In the general approach the whole model is viewed as constructed from similar components, each of them derived from the basic structure described in the previous paragraph. Each component represents cells that are subjected to the same environmental conditions and, therefore behaves similarly (to be denoted *homogenous group*). The whole tumor is modeled as a union of many varying homogenous groups of cells, where the

development of each group can be accurately predicted (when local conditions are known).

This general model simulates progress of the tumor in discrete steps of time. At each step the number of cells in each subcompartment of each group is calculated according to the previous state, parameters of tumor, drug concentration, etc. The parameters of the tumor must include all the information that is relevant to prognosis. Some of these parameters are defined locally, e.g., those relating to the tumor's geometry. For this reason the representation of the spatial structure will be included.

The cells will be able to pass between the groups during the development of the tumor. This allows the representation of the changes in the local conditions during the tumor evolution (e.g. forming of necrotic core, improvement in "living conditions" in vascularized regions, etc.). In addition, all the parameters of the tumor may change in accordance with the dynamics of the cancer.

The calculation of the tumor development over time will be done by stepwise execution of the described simulation and can be used to predict the outcome of the treatment or in fitness function for search algorithms.

2.3. From General to Individual Tumor Model

When the general theoretical description of the model is accomplished, the model is fitted to represent the actual tumors. We render it patient-specific by adjusting all the parameters that determine the behavior of the modeled

tumor to those of the real cancer in the patient's body. In order to accomplish this task we will establish the connections between mathematical parameters (most of them will have direct biological implication) and every kind of data that is practically obtainable in the clinic. These connections may be defined through research on statistic correlation between different parameters (including genotype-phenotype correlation), or using advanced biochemical research (which may establish quantitative relations).

Thus defined, the model will be able to give realistic predictions for treatment outcomes either for specific patient or for a broad range profiles of patients and diseases. This tool can serve to perform the prognosis of either an untreated cancer patient, or as a basis for treatment modeling as is described below.

3. Introducing Pharmacology

In order to simulate cancer treatment we add to the above model the pharmacologic component. We model pharmacokinetics as well as pharmacodynamics for specific anticancer drugs. We begin by representing cell-cycle specific drugs, however the model implies no restriction on the type of drugs to be employed.

We model the distribution of the drug in and around the tumor as well as in the blood (the drug kinetics). For this purpose, we use the suitable model, defining it precisely for every certain type of the drug. The concentrations of drug in the body are calculated at every time step in

60

accordance with the drug administration specified by the protocol, and different processes that define drug kinetics in the body.

The dynamics of the drug are represented through the direct influence of the drug on tumor cells. The effects on the proliferating cells are mostly blocking the cycle in different stages (which can be modeled as cell arrest) and cell death (immediate or after being in the block). Cell-cycle specific drugs are believed to have no direct influence on quiescent cells, but can affect them indirectly by killing proliferative cells and therefore changing local conditions. Where additional types of drugs added to the model, their effect on any kind of cells may be too modeled as killing certain fraction of cells (which is dose-dependent) or changing the behavior of the cells.

Additional phenomena that may prove significant in drug kinetics and dynamics (e.g. rate of absorption by the cells, development of tumor resistance to specific drug, etc.) can be introduced into the model to make it as realistic as needed.

The description of the drug in the model is done in terms of quantitative functions, which enable to calculate the drug amounts at certain locations and the tumor response to it at every time step. In the general case, these functions include parameters that depend on the specific data (drug type, body parameters, characteristic of the tumor, etc.) and can be determined in given situation (patient/case). The relation between clinical data and these parameters can be established in the ways similar to those described for the cancer model.

The combination of cancer model with the drug model described above makes it possible to predict the outcome of the treatment, given the relevant

parameters for the drug, the cancer and the patient. Again, the prognosis may be made for specified cases as well as for broad profiles of patients or disease. This simulation also serves to build the fitness function used for the optimaization objectives.

5

4. Combining with minimizing host toxicity.

Although an accurate predictive tool, the model that represents chemotherapy of tumor alone cannot be used in optimization, for it posts no constraint on the choosing of the treatment. Actually, this model implies using as much drug as possible until the final elimination of the tumor; while in the live system the toxicity of the drug is the most important constraint limiting the treatment. In most cases of anticancer chemotherapy the dose-limiting toxicity is bone marrow suppression, the two most sensitive bone marrow lineages being granulopoiesis and thrombopoiesis. Accordingly, those two were chosen as an example and are modeled separately and in a similar way to predict the negative effect of the chemotherapy on them. These models reconstruct the damage caused by the chemotherapy to the bone marrow cells and the recovery of these lineages (treated by specific growth factors).

Thus, the whole system is capable of predicting the result of chemotherapy treatment for the tumor as well as for bone marrow cells, allowing the use of the protocols that combine anticancer drugs and growth factors for healthy cells.

Chemotherapy toxicity to any other normal host cell population can be similarly taken into account, if it is defined as relevant for dose and schedule optimization.

5

VI. INDIVIDUALIZATION OF THE MODELS

Due to a great degree of heterogeneity between malignant tumors (even among similar tissue types) and between patients, it would be advantageous to adjust the treatment protocol to the individual case. This individualization

10 procedure includes three aspects:

1) individual parameters of tumor dynamics

2) individual parameters of patient-specific drug pharmacokinetics

3) individual parameters of the dynamics of dose-limiting normal host tissues.

15 Relevant data concerning individual cases can be obtained by research on statistic correlation between different parameters (including genotype-phenotype correlation), or using advanced biochemical research (which may establish quantitative relations). In the general model, important dynamic parameters are estimated from experimental studies conducted in certain

20 patient populations. Any of these parameters, when available on the per patient basis, can be individualized, while those that are unavailable can be left as a population-based figure. This approach allows continuous increase in the degree of individualization of the treatment protocols with progress in the technology of parameter evaluation (e.g., oncochips).

All different parameters may then be adjusted, which will result in an adjusted array of models to be simulated. Parameters may include many different factors, which are adjustable according to the needs of a pharmaceutical company for general use of the treatment, or may even be individualized for use by a specific clinician for a particular individual. Examples of parameters may include, but are not limited to age, weight, gender, previous reaction to treatment, desired percentage of healthy body cells, desired length of treatment protocol, pathologic or cytologic specifics, molecular markers, genetic markers etc.

In order for the system to be user-friendly, all possible parameters are termed in ways that are easy for the user to understand.

Once all the parameters are set, an array of solutions is produced based on the input parameters. A number of possible protocols can be set (is thus generated by the computer). a fitness function is applied, which results in scores for each of the proposed solutions.

GENERATION OF PROTOCOL SPACE

Refer back to Fig. 2. This model makes it possible to check any given treatment protocol and to choose a very good one according to user's criteria. The user may be a physician, a drug developer, a scientist, or anyone else who may need to determine a treatment protocol for a drug. The specific parameters may include several categories, such as individual patient characteristics and/or medical history, needs of a specific user (research,

efficacy, treatment, etc.), and other particulars (such as maximum length of treatment, confidence level, etc.).

. That is, an array of possible treatment protocols is created from which
5   the optimal treatment protocol can then be chosen. It should be noted that the method does not imply the fitness estimation for all possible protocols. The use of operation research allows a much more sophisticated, yet resource saving procedure.

An example of this procedure will be described as it relates to cancer
10 treatment by chemotherapy, as described in the third embodiment of the invention above. However, it should be noted that a similar procedure may be performed in any of the embodiments.

The procedure implements cell growth and cell death procedures, as defined in the detailed model above.   There are certain pre-defined
15 parameters, including the lengths of the host and target life-cycles, the lengths of their critical phases, and a resolution factor, that determines the length of a single time unit. The user is asked to define an action (treatment or non-treatment). Simulation of cell growth and death is then performed for the single time unit.   This procedure is repeated until the end of the total
20 simulation. Alternatively, the choice of treatment or non-treatment is made by the processor, with many possible permutations considered. In that case, the protocol space would be very large, and the resolution would depend on the (selected) length of the time unit (and computer capacity)

65

There are two procedures: one for growth simulation during treatment and one without. The array in which the numbers of cells are kept is updated once per time unit, whether with or without treatment present at that time.

5

VII. Defining the Fitness Function

The fitness function is an important tool in Operation Research. In this case of protocol optimization, it allows the comparison between a number of different protocols each one of them scoring differently with respect to various

10   objectives that can be set by the developers or by the users and identifying the protocol for which the highest weighted score is predicted. The fitness function calculates for any given protocol its relative efficacy ("score" or "fitness"), thus enabling a definite decision of the best protocol from a given set of protocols.

15   In different cases, different objectives can be formulated. There are several settings in which such a model can be used, including but not limited to:

One) clinical practice- where objectives can change depending on type of disease, condition of the patient, purpose of treatment, etc.

20   Two) pharmaceutical company- where objectives can be aimed at finding the therapeutic window and an optimal schedule.

Three)scientific setting- research oriented objectives can be aimed at.

In each case, a particular fitness function can be formulated, reflecting all given requirements. Thus, in any particular case one can compare

between different protocols and obtain the most suitable to his/her special purposes and needs.

Examples for some alternative objectives are given:

1. The smallest number of drug dosings required for achieving any given aim.

2. The lowest total drug dose required for achieving any given aim.

3. The minimal total amount of drug needed for rehabilitation.

4. The smallest deviation from the baseline at normal cell population count (e.g., platlet nadir) after chemotherapy or another cell-suppressive treatment.

5. The shortest period of disease (e. g.,thrombocytopenia).

Using the fitness function it is possible to a) estimate the efficacy of a given protocol, b) search for the solution of an optimization problem, i.e., predict which protocol will be best of many potential protocols considered for curing/relieving the patient.

VIII. Solving the Optimization Problem

The optimization problem is stated using the described models: to find the protocol for drug administration (with option to growth factor administration) which maximizes the given fitness function.

As explained above, we define the fitness function according to the user requirements. For example, the goal of the treatment may be defined as minimizing the number of cancer cells at the end of the treatment, minimizing

the damage to the BM cells throughout the treatment or at its end, and curing

the patient (where cure is defined precisely) as quickly as possible. Note that

the fitness function may also include goals such as maximizing life

expectancy, minimizing cost of treatment, minimizing treatment hazards

5   and/or discomfort etc. Generally, the aim of optimization is to find the best

protocol, i.e. the protocol that generates the best value of fitness.

Customarily, this is achieved by mathematical analysis. However,

mathematical analysis is restricted to over simplified models, whereas, in

order to accommodate biologically realistic parameters, the described models

10   are very complex and, therefore, cannot be solved analytically. On the other

hand, the practical purpose of the treatment is not to find *the best possible*

protocol (i.e., the global optimum) but "only" one that will suit the user's

objectives, even if its fitness is not absolutely the best (i.e., the local

optimum). For this reason we can be satisfied with the solution that can be

15   shown to promise the pre-defined objectives.

       Hence, the optimization problem may be reformulated as follows: for

given initial conditions, find the treatment protocol which will fulfill the user's

requirements (e.g. curing a patient according to given definitions of cure) and

subjected to given limitations (e.g. treatment duration, drug amounts, etc.). To

20   this end it is not compulsory to find **the** global solution. It is enough, with

regards to objectives and limitations, to perform search, using search

algorithms, in certain regions of the protocols' space, and find the local

maxima of the fitness function. After determining the locally best protocols, we

can verify that they serve one's objectives and check them numerically for

25   stability.

Such a strategy can be used for identifying patient-specific treatment, as well as in the general case, where only the profile of the disease and the drug are specified. If more patient-specific data are supplied, the solution will be tailored more specifically. On the other hand, the optimization program could propose general recommendations for the protocol types for certain kinds of disease, treated with a certain kind of medication.

It will be appreciated that the present invention is not limited by what has been described hereinabove and that numerous modifications, all of which fall within the scope of the present invention, exist. For example, while the present invention has been described with respect to certain specific cell lineages, the concept can be extended to any other lineage and treatment protocol which can be detailed mathematically (e.g., viral or bacterial diseases). Furthermore, certain assumptions were necessarily used in computing the mathematical models of the embodiments. Values and equations based on these assumptions can be changed if new information becomes available.

It will be appreciated by persons skilled in the art that the present invention is not limited by what has been particularly shown and described herein above. Rather the scope of the invention is defined by the claims which follow:

What is claimed is: **[independent claims listed now, dependent claims to follow] (Note that we are not in a position to revise the claims. Z. Agur)**

1. A system for individualized optimization of a treatment protocol, the system comprising:

5   a system model comprising:

a model of a biological process; and

a mathematical model of treatment effects on said biological process;

a plurality of treatment protocols;

10   means for adding individualized parameters to said system model, whereby said system model is modified based on said individualized parameters; and

a selector for selecting an optimal treatment protocol from said plurality of treatment protocols based on modification of said system model.

15   2. A system for identification of optimal treatment protocols using heuristic analysis, the system comprising:

a biological model;

a plurality of treatment protocols included within said model, thereby providing a plurality of treatment models, wherein said treatment models
20   provide effects of said treatment protocols on said biological model; and

heuristic means for identification of said optimal treatment protocol from said treatment models.

70

What is claimed is: **[independent claims listed now, dependent claims to follow]** (**Note that we are not in a position to revise the claims. Z. Agur**)

1. A system for individualized optimization of a treatment protocol, the system comprising:

5   a system model comprising:

          a model of a biological process; and

          a mathematical model of treatment effects on said biological process;

          a plurality of treatment protocols;

10   means for adding individualized parameters to said system model,

whereby said system model is modified based on said individualized parameters; and

          a selector for selecting an optimal treatment protocol from said plurality of treatment protocols based on modification of said system model.

15   2. A system for identification of optimal treatment protocols using heuristic analysis, the system comprising:

          a biological model;

          a plurality of treatment protocols included within said model, thereby providing a plurality of treatment models, wherein said treatment models

20   provide effects of said treatment protocols on said biological model; and

          heuristic means for identification of said optimal treatment protocol from said treatment models.

3. A system for presenting a individualized model of a biological process, the system comprising:

a processor for generating a model of a biological process;

a plurality of experimental data, included within said model; and

means for including individual data into said processor, thereby providing said individualized model of said biological process.

4. A system for prediction of outcomes of a treatment protocol, the system comprising:

5. A system for describing treatment effects on a biological process

6. A method for individualized optimization of treatment, the method comprising the steps of:

providing a biological model;

inputting parameters into said model;

computing treatment protocols for said model within said parameters;

applying a fitness function to said treatment protocols; and

choosing an optimal treatment protocol based on said fitness function.

7. A method for optimization of a treatment protocol, the method comprising the steps of:

providing a variable representing an amount of medication administered;

providing behavior characteristics of said administered medication;

providing a model of a cell line predicting effects of said administered medication on said cell line;

calculating a .....

determining a treatment protocol

8. * A system for prediction of outcomes of treatment of thrombocytopenia by Thrombopoietin (TPO), the system comprising:

9. * A system for prediction of outcomes of treatment of neutropenia with Granulocyte colony stimulating factor.

10. A system for individualized optimization of treatment of neutropenia, the system comprising:

   a system model comprising:

   a mathematical model of a neutrophil lineage; and

   a mathematical model of effects of treatment on said neutrophil lineage;

   a plurality of treatment protocols;

   means for adding individualized parameters to said system model, whereby said system model is modified based on said individualized parameters; and

   a selector for selecting an optimal treatment protocol from said plurality of treatment protocols based on modification of said system model.
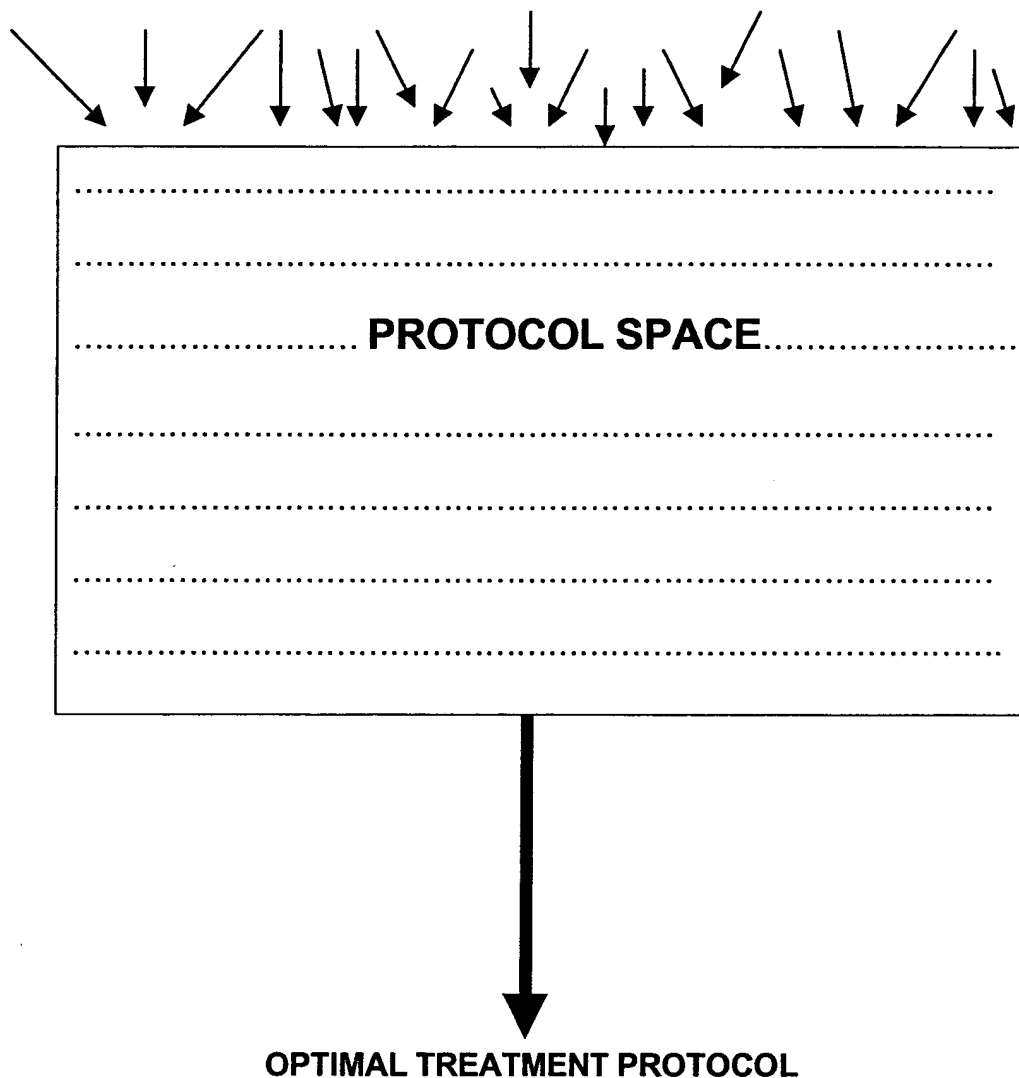
11.

CONCEPT

5

DETAILED PARAMETERS

PROTOCOL SPACE

10

OPTIMAL TREATMENT PROTOCOL

Fig. 1

15

1.1   1.2   **METHODOLOGY**   1.3

```
┌─────────────────────┐  ┌─────────────────────┐  ┌─────────────────────┐
│ MODEL BIOLOGICAL    │  │ PATIENT-SPEC.       │  │ MODEL TREATMENT     │
│ PROCESS- GENERAL    │  │ CLINICAL            │  │ EFFECTS             │
│ (population mean     │  │ PARAMETERS          │  │                     │
│ parameters)         │  │ (ambulatory)        │  │                     │
└─────────────────────┘  └─────────────────────┘  └─────────────────────┘
```

10

15

The biological process can
be general or patient
tailored

```
        ┌──────────────┐
        │  COMPLETE    │
        │  DETAILED    │
        │  MODEL       │
        └──────────────┘
```
1.4

20

25

1.5   PROTOCOL
       SPACE

INPUT SCENARIO PARAMETERS   These
parameters (dosing intervals, dosing
duration, drug quantity...) are actually
not inputed by the user. The computer
generates the protocol space by itself.

30

```
        ┌──────────────┐
        │ APPLY FITNESS│
        │ FUNCTION     │
        └──────────────┘
```
35   1.6

```
        ┌──────────────┐
        │SEARCH HEURISTICS│
        │(OPTIMIZATION)  │
        └──────────────┘
```
40

1.7

**DEFINE SPECIFIC
PARAMETERS**
User's objectives

45

```
        ┌──────────────┐
        │  OPTIMAL     │
1.8     │  TREATMENT   │
        │  PROTOCOL    │
        └──────────────┘
```

50

Fig. 2

75

Attempting to optimize some instance of a chemotherapy problem with a given set of solutions...

Fig. 2a

Fig 3

Fig 4

Fig 5

5
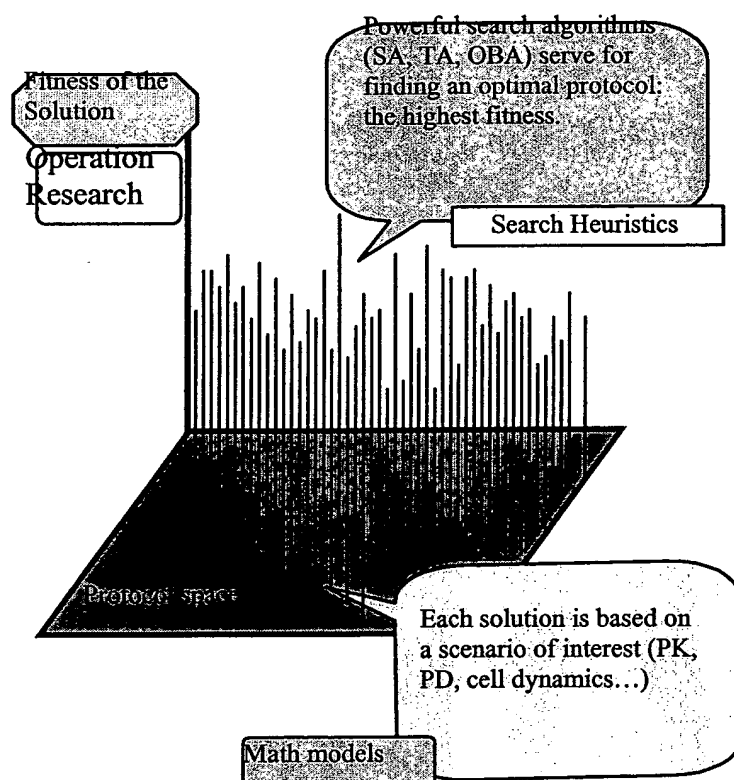
Time (hrs) / Compartment	0	1	2	3	4	5	6	7	8	9	10	.	.	.	.	.	.	.	.	.	.	.	.
SC											→												
CFU											→												
1KB											→												
MK16											→												
MK32											→												
MK64											→												
MK128											→												
PL											→												
TPO											→												

10

15

20

25

30
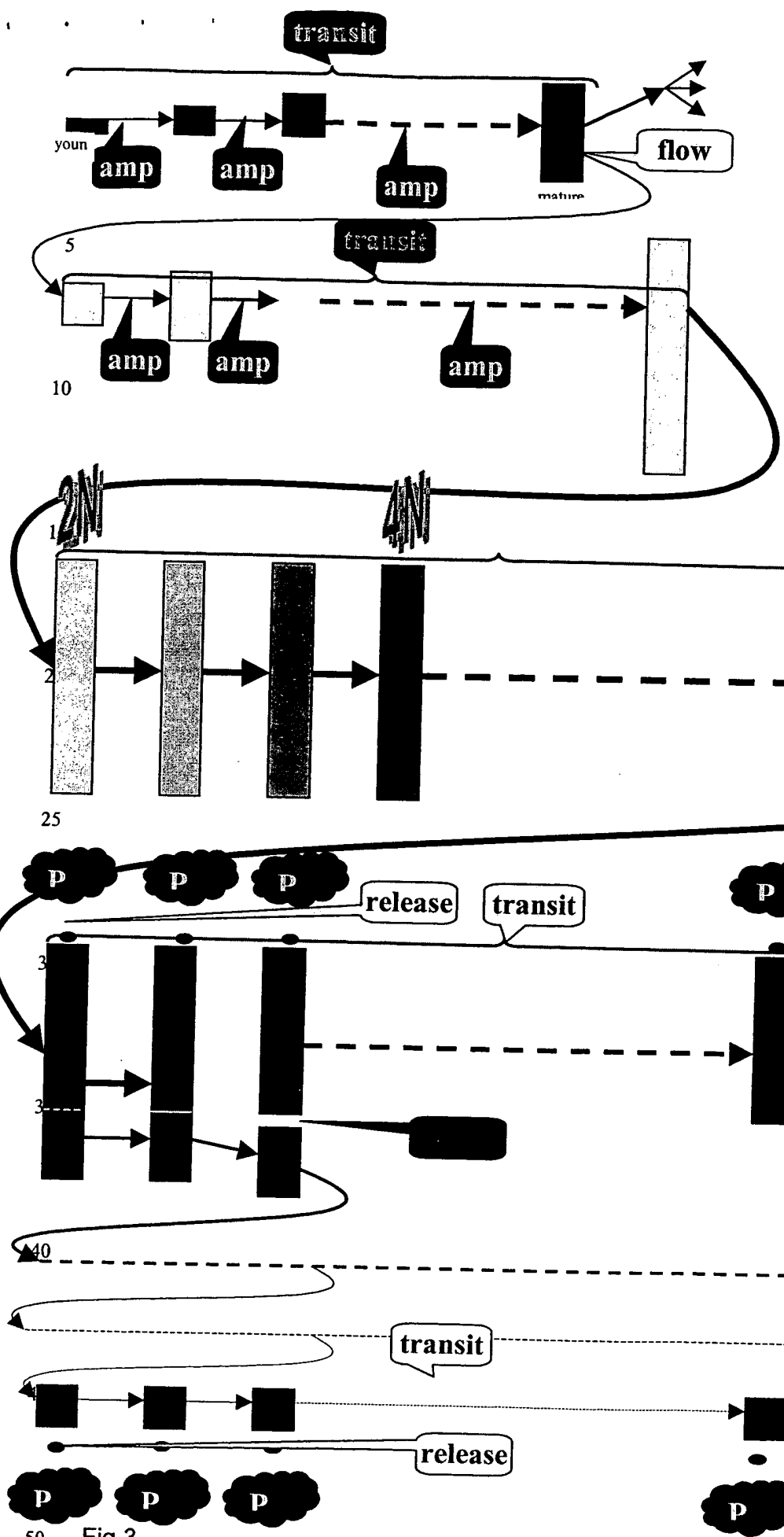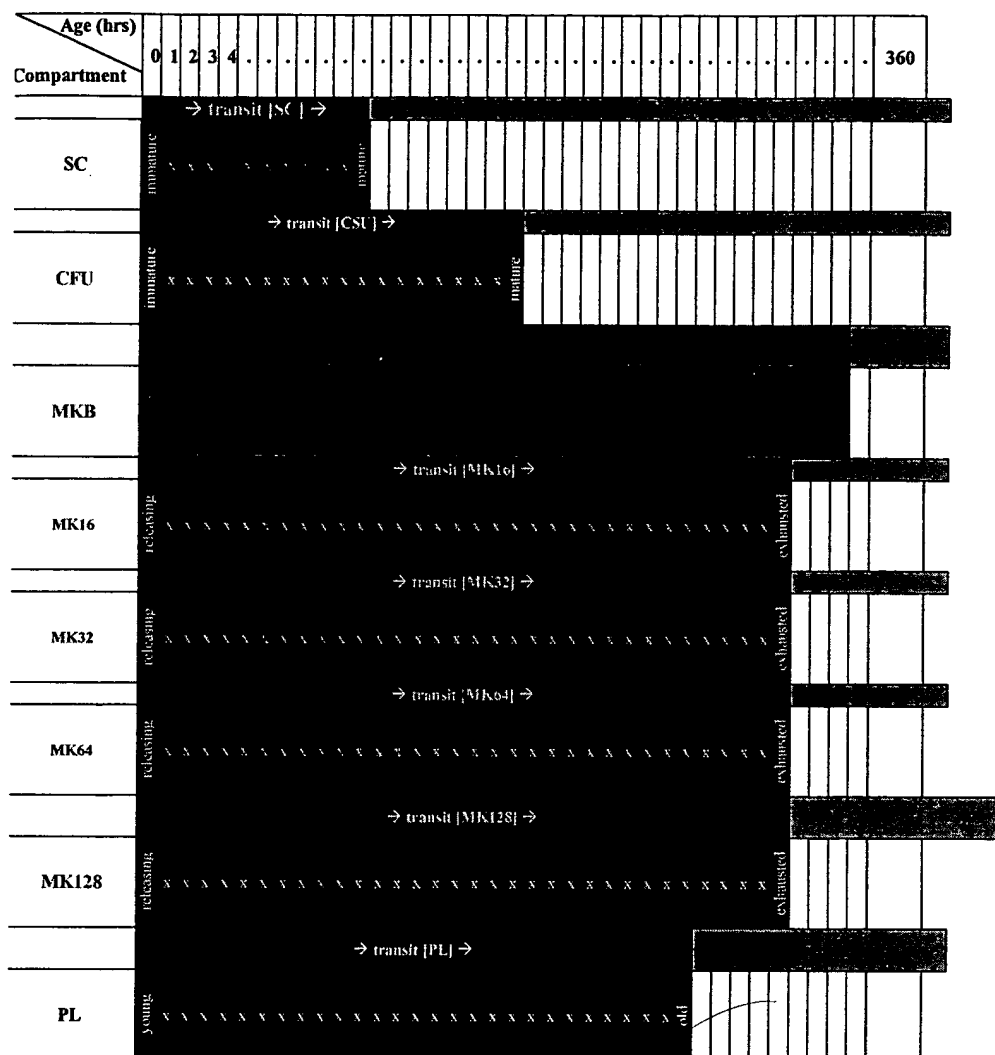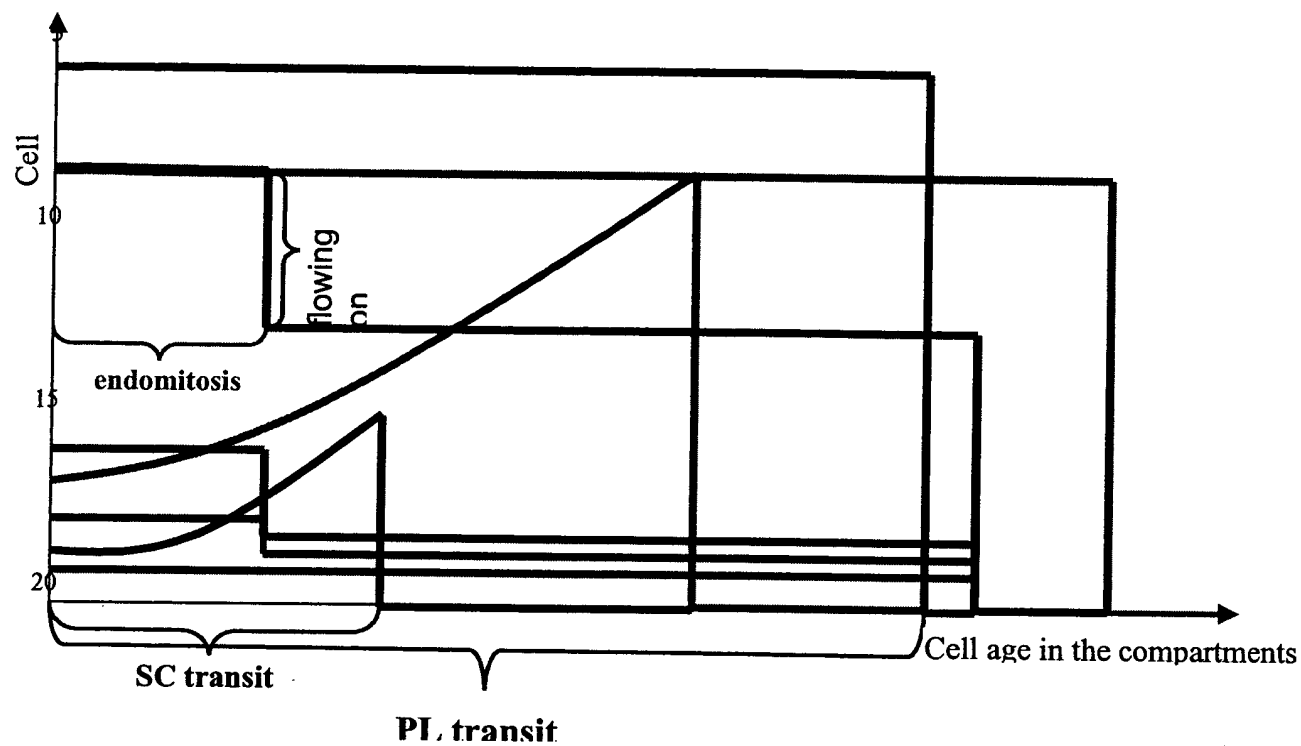
Fig. 6

5

10

15

20

25   Fig 7

81
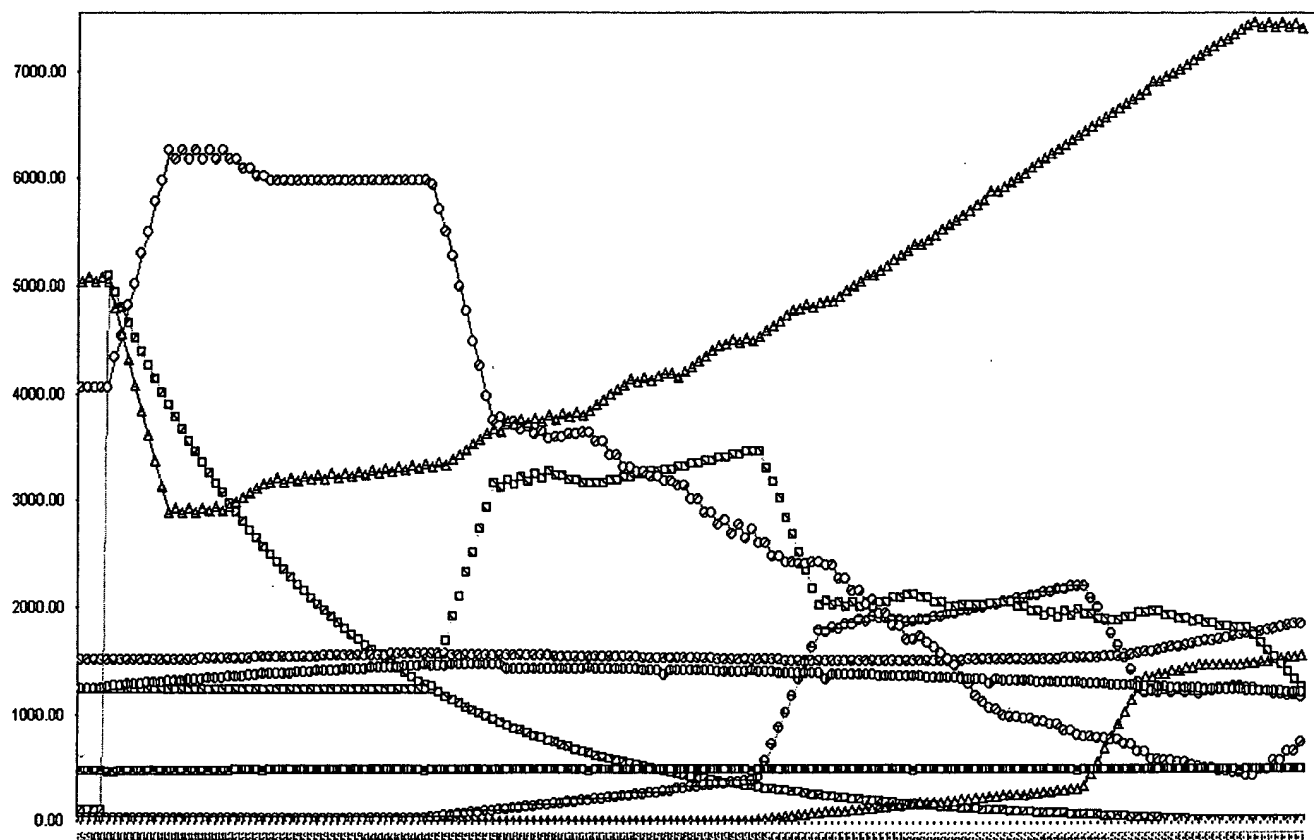
Simulations showing that if the protocol is pre-calculated then a similar or a higher efficacy can be obtained using 4-fold reduced total dose of TPO.

5

TPO use in healthy donors:
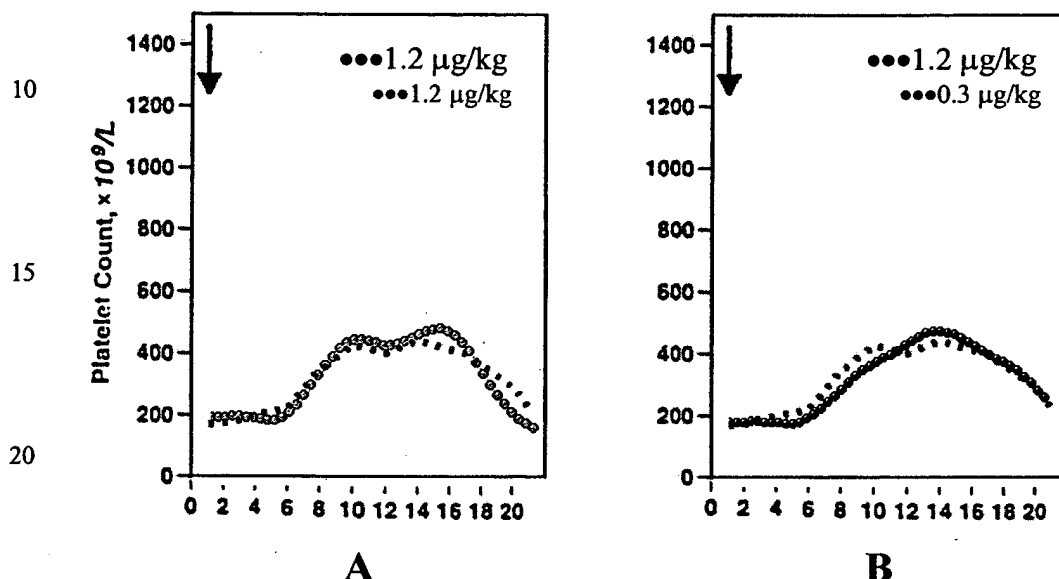

A   B

Fig. 8: TPO given to healthy donors- Results of TPO clinical trials from recent research on healthy platelet donors, as
25 compared to our computer simulation results. Arrows indicate the start of TPO treatment. (A) Comparison of experimental data from published articles[1] (black) and our model simulation (green), in both TPO was given as a single IV dose of 1.2 μg/kg on day 0. (B) Comparison of the same experimental data (black) and our proposed TPO administration protocol; the total dose in the simulated protocol was 0.3 μg/kg (blue).
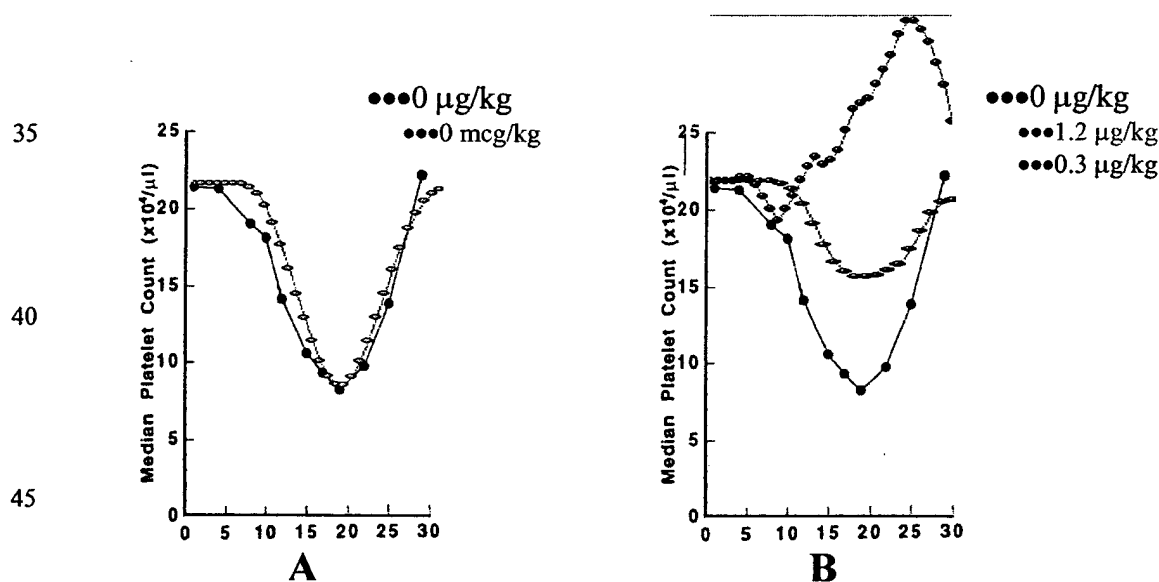
TPO use in patients receiving chemotherapy:

A   B

Fig. 9: TPO with chemotherapy- (A) Results of clinical trials from recent research on thrombocytopenia induced in patients
50 receiving single carboplatin chemotherapy[2] on day 0 (black), as compared to our model simulation of these results (green). (B) The same experimental data (black); simulations of the same experiment, with addition of "conventional" TPO protocol of a single IV dose of 1.2 μg/kg on day 0 (olive); simulations of the same experiment under our proposed protocol that totals
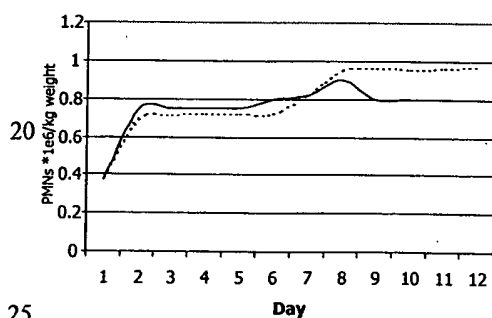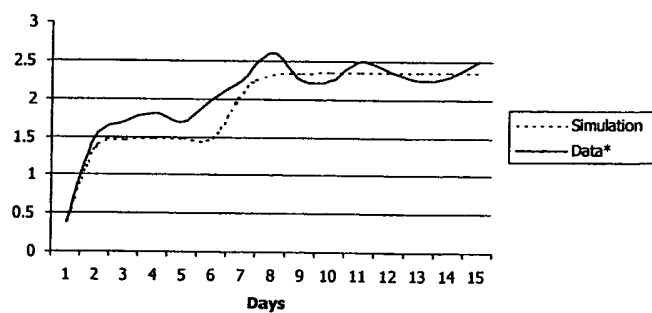
83

5

10

Fig 11

15

20
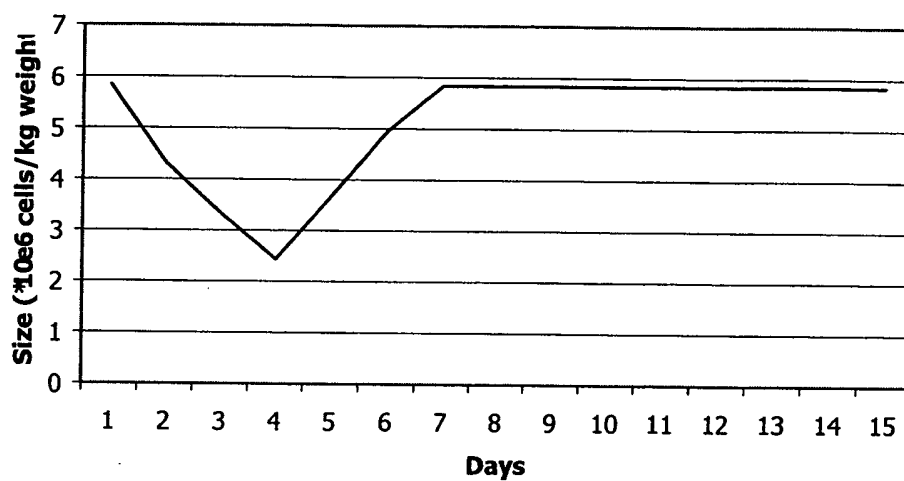
25

Fig 12a

Fig 12b

30

Optimizing cytotoxic drug delivery (administration/efficacy) for cancer patients

Introduction

Cancer is the second leading cause of mortality in the US, resulting in approximately 550,000 deaths a year. There has been a significant overall rise in cancer cases in recent years, attributable to the aging of the population. Another contributing factor to the rise in the verifiable number of cases is the wider use of screening tests, such as mammography and elevated levels of prostate specific antigen (PSA) in the blood.

Neither better detection nor the natural phenomenon of aging, however, can entirely explain the increase in new cases of tumors. Meanwhile, other cancers, like brain tumors and non-Hodgkin's lymphoma, are becoming more common. Their increase could reflect changes in exposures to as yet unidentified carcinogens. Current trends suggest that cancer may overtake heart disease as the nation's no. 1 killer in the foreseeable future. As gene therapy still faces significant hurdles before it becomes an established therapeutic strategy, present control of cancer depends entirely on chemotherapeutic methods.

Chemotherapy is treatment with drugs to destroy cancer cells. There are more than 50 drugs that are now used to delay or stop the growth of cancer. More than a dozen cancers that formerly were fatal are now treatable, prolonging patients' lives with chemotherapy.

Treatment is performed using agents that are widely non-cancer-specific, killing cells that have a high proliferation rate. Therefore, in addition to the malignant cells, most chemotherapeutic agents also cause severe side-effects because of the damage inflicted on normal body cells. Many patients develop severe nausea and vomiting, become very tired, and lose their hair temporarily. Special drugs are given to alleviate some of these symptoms, particularly the nausea and vomiting. Chemotherapeutic drugs are usually given in combination with one another or in a particular sequence for a relatively short time.

Chemotherapy is a problem involving many interactive nonlinear processes which operate on different organizational levels of the biological system. It usually involves genomic dynamics, namely, point mutations, gene amplification or other changes on the genomic level, which may result in increasing virulence of the neoplasia, or in the emergence of drug resistance. Chemotherapy may affect many events on the cellular level, such as cell-cycle arrest at different checkpoints, cell transition in and out of the proliferation cycle, etc. Chemotherapy may also interfere with the function of entire organs, most notably, with bone marrow blood production. In recent years molecular biology and genetics has made an important step forward in documenting many of these processes. Yet, for assessing the contribution of specific molecular elements to the great variety of disease profiles, experimental biology must be provided with tools that allow a formal and systematic analysis of the intricate interaction between the genomic, cellular and cell population processes in the host and in the disease agent.

This system is so complex that there is no intuitive way to know how small changes in the drug protocol will affect prognosis. But in spite of this intricacy, attempts to improve chemotherapy have been carried out by "trial and error" alone, with no formal theory underlying the application of specific drug schedules. Such an approach "is apt to result in no improvement, only discouragement and little useful information for future planning" (Skipper, 1986).

1. General Description

The product is a method for identifying clinically feasible and efficacious optimal treatment protocols for anticancer drugs. We do this by using (1) optimization methods taken from Operation Research, and involving heuristic search algorithms. These are applied for (2) testing the performance of a very large number of drug protocols on (3) "virtual cancer patients," in the form of realistic computer simulations of detailed mathematical models of the involved dynamics. **Our method is the first which can identify optimal treatment protocols, without any constraint on the level of complexity of the mathematical models of the biological, clinical and pharmaceutical processes. This means that the description of the system can be as realistic as required.** Previous optimization methods imposed constraints on the level of complexity of the mathematical methods, so that the simulated systems were always too simplistic to retrieve the clinical situation.

The assumption that underlies this method is, that the effect of a certain drug on a certain cancer cells population depends on the overall population dynamics of the tumor. To describe these complicated dynamics we use a set of models that follow up the changes in cancer cell numbers, spatial distribution and other relevant phenotypic (epigenetic) factors, taking into consideration also the genetic profile of the patient, in cases where this one is available. To also allow for the use of cell-cycle-phase-specific drugs, we follow-up each drug susceptible body cell (normal and cancer) according to its cell-cycle status. Because any realistic description of such "virtual patient" is too complex to be attacked by analytical optimization method, then our introduction of the heuristic optimization methods approach is a highly significant novelty.

The project consists of 6 successive stages:

1) Developing the appropriate mathematical models to describe the cancer cell populations with respect to the cell-cycle as well as spatio-temporal dynamics. This model can be as complex as necessary for enabling an accurate computation of the number of cancer cells at any given moment.

2) Inputting individual parameters into the model and, hence, bridging between the model and accessible clinical data regarding profiles of the tumor and of the patient.

3) Introducing drug characteristics (mode of action, effect and on tumor cells etc.), the pharmacokinetics and the pharmacodynamics into the model, using experimental data about the relevant drugs.

4) Combining this model with additional models that consider toxic effects of the drug on the host (e.g., granulocytic and thrombocytic lineages).

2

5) Defining a general fitness function for given protocol, so that this system may serve as prediction tool for anticancer treatment (with an option of tuning by the user).

6) Using search algorithms and computer simulations to search through the possible protocols space in order to obtain the best/most suitable solution.

The search process may be performed on several levels, starting from the most general (for a given type of disease), to the most detailed and patient-specific level (which will require relevant clinical data about the patient). In the case of a more generalized search, the certain region of protocols may be proposed as most suitable for given type/profile of cancer; in the case of specified search, this region can be narrowed according to additional patient data.

2. Mathematical Model:

2.1. Basic Tumor Layer

The basic layer of the model incorporates a description of age distribution of cycling cells and number of resting (quiescent) cells. The term "age of the cell" here refers to chronological age starting from the conventional beginning point of mitotic cycle.

In what follows we give the definition of this basic model:

- The whole cycle is divided into 4 compartments, or *stages* (G_1, S, G_2 and M). Each compartment is divided into equal *subcompartments*, where i^{th} *subcompartment* in each stage represents cells of age i in this stage (i.e. they have spent i time-steps in this stage).
- Let $\{G_1, S, G_2, M\}$ denote the corresponding stages of the cell cycle, and G_0 – the quiescence.
- Let T_k denote the maximum duration of kth stage in the cycle.
- We denote as • t the time resolution of the model – discrete time steps.

- $x_k^i(t)$ is a function which represents the number of cells in stage k with age i into this stage, at time t to $t+$• t. Both time and age are measured in same units (hours).
- $Q(t)$ represents the number of resting cells at time t to $t+$• t.
- *Trans(k,i,t)* represents the probability that a cell of age i in the stage k will move to the next $(k+1)$ compartment. Cells entering the new stage always start from the first subcompartment, i.e. from $i=1$. This probability may change with time.
By definition: $\forall k : Trans(k, T_k) = 1$ That means that the cell cannot remain more than T_k in k compartment.
- Let T_0 *and* T_R denote the onset of G1 and the age at which the cell passes through R-point (*restriction point*) in G1, respectively. The later is associated with commitment to complete the mitotic cycle.
- The total number of proliferating cells $P(t)$ can be calculated as follows:

$$P(t) = \sum_{k=G1,S,G2,M} \left(\sum_{i=1}^{T_k} x_k^i(t) \right)$$

3

- In every time interval, quiescent cells may return to the proliferation pool. Alternatively proliferating cells may change their state to become quiescent if they are in G1 stage and at age i, where $T_R \cdot i > 0$. To describe this process we introduce the function $G_{1 \cdot 0}(i,t)$ which describes the number of G1 cells in age i which become quiescent, during time interval $[t, t+ \cdot t]$. This function may receive negative values, accounting for cells that return from resting to proliferation.

As we assume that the exit to quiescence can occur only prior to the R-checkpoint (even in cancer cells), and that a resting cell which returns to proliferation enters the cycle at T_0, it can be stated:

$$\forall i > T_R, \forall t : G_{1 \to 0}(i,t) = 0$$

It must be noted, that this function is not dependent on i and t solely. Its value is determined according to current cell distribution and all the general parameters that characterize the described cells group. The same should be said about the values of *Trans* vector that can change during the history of given population.

- The model traces the development of described group of cancer cells using given parameters, by calculating the number of cells in each and every subcompartment according to the following stepwise equations:

$$x_k^i(t) = \begin{cases} x_k^{i-1}(t-1) \cdot [1 - Trans(k, i-1, t-1)], & 1 < i \leq T_k \\ \\ \sum_{j=1}^{T_{k-1}} [x_{k-1}^j(t-1) \cdot Trans(k-1, j, t-1)], & i = 1 \end{cases}$$

$$x_s^i(t) = \begin{cases} x_s^{i-1}(t-1) \cdot [1 - Trans(S, i-1, t-1)], & 1 < i \leq T_{G1} \\ \text{for } k = G_2, M, \ k-1 \text{ returns the previous stage (e.g. } G_2 \text{-} 1 = S). \\ \\ \sum_{j=1}^{T_{G1}} [x_{G1}^j(t-1) \cdot Trans(G1, j, t-1)] \cdot [1 - G_{1 \to 0}(i-1, t-1), & i = 1 \end{cases}$$

$$x_{G1}^i(t) = \begin{cases} x_{G1}^{i-1}(t-1) \cdot [1 - Trans(G1, i-1, t-1)] \cdot [1 - G_{1 \to 0}(i-1, t-1)], & 1 < i \leq T_{G1} \\ \\ 2 \cdot \{\sum_{j=1}^{T_M} [x_M^j(t-1) \cdot Trans(M, j, t-1)]\}, & i = 1 \end{cases}$$

- These equations make it possible to calculate the number of cells in each subcompartment at every time interval $[t, \cdot t]$ starting from initial distribution (e.g. at time $t=0$).

Remarks:

1) As stated above, cells ages are measured in absolute time units, and therefore refer to the chronological age of the cell (as opposed to biological age, which refers to maturity of the cell and its units are relative to maturation rate that is different from cell to cell). As a consequence, in this model no cell can remain in the same age subcompartment after every time step. On the other hand, a fraction of the cells that leaves any subcompartment may be transferred to the first subcompartment of the

next stage, according to probability vector *Trans(k,i,t)*. This fact enables us to account for variability of cycle lengths while retaining deterministic approach.

2) The behavior of the cell population in this model is wholly controlled by two components: *Trans* vector, and *G1toG0* function. These two functions determine uniquely the outcome of every single time step, and, consequently the result over the long periods. We name them here "*control functions*". As we have mentioned, the values of these functions may be dependent not only on time and age of cells, but also on the current population state (or, generally, on the whole history of the population) as well as on the environment associated with given cells group. On the other hand, those parameters are similar for all the cells in the group. This implies that the model presented here is suitable for describing highly homogenous group of cells. As it will be claimed later, control functions values are determined by the parameters that describe the local conditions for given population. Therefore, we expect the basic layer of the model to give realistic description of uniform group of cancer cells for which environmental conditions and relevant biological properties are defined, in a way that will allow the construction of the control functions for this group.

2.2. The General Tumor Model

In the general approach the whole model is viewed as constructed from similar components, each of them derived from the basic structure described in the previous paragraph. Each component represents cells that are situated in the same environmental conditions and, therefore behaves similarly. We call them *groups*. The whole tumor is modeled as union of heterogeneous groups of cells, where the development of every group can be accurately predicted (when local conditions are known).

This general model simulates progress of tumor in time by discrete steps. At each step the number of cells in each subcompartment of each group is calculated according to the previous state, parameters of tumor, drug concentration, etc. The parameters of the tumor must include all the information that is relevant to the prognosis. Some of these parameters are defined locally, e.g., those relating to the tumor 's geometry. For this reason the representation of the spatial structure will be included.

The cells will be able to pass between the groups during the development of the tumor. This allows the representation of the changes in the local conditions, during the tumor evolution (e.g. forming of necrotic core, improvement in "living conditions" in vascularized regions, etc.). In addition, all the parameters of the tumor may change in accordance with the dynamics of the cancer.

The calculation of the tumor development over time will be done by stepwise execution of the described simulation and can be used to predict the outcome of the treatment or in fitness function for search algorithms.

2.3. From General to Individual Tumor Model

When the general theoretical description of the model is accomplished, the model is fitted to represent the actual tumors. We render it patient-specific by adjusting all the parameters that determine the behavior of the modeled tumor to those of the real cancer in the patient's body. In order to accomplish this task we will establish the

connections between mathematical parameters (most of them will have direct biological implication) and every kind of data that is practically obtainable in the clinic. This individualization procedure includes three aspects:

1) individual parameters of tumor dynamics
2) individual parameters of specific drug pharmacokinetics for a specific patient.
3) individual parameters of the dynamics of dose-limiting normal host tissues.

These connections may be defined through research on statistic correlation between different parameters (including genotype-phenotype correlation), or using advanced biochemical research (which may establish quantitative relations).

In the general model important dynamic parameters are estimated from experimental studies that are conducted in certain patient populations. Any of these parameters, when available on the per patient basis, can be individualized, while others left as population-based means. This approach allows continuous increase in the degree of individualization of the treatment protocols with progress in the technology.

Defined so, the model will be able to give realistic predictions for treatment outcome either for specific patient or for a broad range profiles of patients and diseases. This tool can serve to perform the prognosis of an untreated cancer patient, or as a basis for treatment modeling.

3. Introducing Pharmacology

In order to simulate cancer treatment we add to this model the pharmacologic component. We model pharmacokinetics as well as pharmacodynamics for specific anticancer drugs. We begin by representing cell-cycle specific drugs, however the model implies no restriction on the type of drugs to be employed.

We model the distribution of the drug in and around the tumor as well as in the blood (the drug kinetics). For this purpose, we use the suitable model, defining it precisely for every certain type of the drug. The concentrations of drug in the body are calculated at every time step in accordance with the drug administration specified by the protocol.

The dynamics of the drug are represented through the direct influence of the drug on tumor cells. The effects on the proliferating cells are mostly blocking the cycle in different stages (which can be modeled as cell arrest) and cell death (immediate or after being in the block). Cell-cycle specific drugs have no direct influence on quiescent cells, but can affect them indirectly by killing proliferative cells and therefor changing local conditions. Where additional types of drugs added to the model, their effect on any kind of cells may be too modeled as killing certain fraction of cells (which is dose-dependent) or changing the behavior of the cells.

Additional phenomena that may come out to be significant in drug kinetics and dynamics (e.g. rate of absorption by the cells, development of tumour resistance to specific drug, etc.) can be introduced into the model to make it as realistic as needed.

The description of the drug in the model is done in terms of quantitative functions, which enable to calculate the drug amounts at certain locations and the tumor response to it at every time step. In the general case, these functions include parameters that depend on the specific data (drug type, body parameters, characteristic of the tumor, etc.) and can be determined in given situation. The relation between clinical data and these parameters can be established in the ways similar to those described for the cancer model.

The combination of cancer model with the drug model described above makes it possible to predict the outcome of the treatment, given the relevant parameters for the

drug, the cancer and the patient. Again, the prognosis may be made for specified cases as well as for broad profiles of patients or disease. This simulation also serves to build the fitness function used in search algorithms in optimization system.

4. Combining with minimizing host toxicity.

Although being accurate predictive tool, the model that represents chemotherapy of tumor alone cannot be used in optimization, for it posts no constraint on the choosing of the treatment. Actually, this model implies using as much drug as it is possible until the final elimination of the tumor; while in the live system the toxicity of the drug is the most important constraint limiting the treatment. In most cases of anticancer chemotherapy the dose-limiting toxicity is bone marrow suppression, the two most sensitive bone marrow lineages being granulopoiesis and thrombopoiesis. Accordingly, those two were chosen as an example and are modeled separately and in the similar way to predict the negative effect of the chemotherapy on them. These models reconstruct the damage caused by the chemotherapy to the bone marrow cells and the recovery of these lineages (also treated by specific growth factors).

Thus, the whole system is able to predict the result of chemotherapy treatment for the tumor as well as for bone marrow cells, allowing the use of the protocols that combine anticancer drugs and growth factors for healthy cells.

Chemotherapy toxicity to any other normal host cell population can be similarly taken into account, if it is proven to be relevant for dose and schedule optimization.

5. Defining the Fitness Function

Fitness function is an important tool in operation research. In the method developed by us it allows the comparison between a number of different protocols each one of them scoring differently with respect to various objectives that can be set by the developers or by the users and identifying the protocol for which we predict the best weighted score. Fitness function calculates for any given protocol its relative efficacy, thus enabling a definite decision of the best protocol from a given set of protocols.

In different cases, different objectives can be formulated. There are 3 main settings in which such a model can be used:

One) clinical practice- where objectives can change depending on type of disease, condition of the patient, purpose of treatment, etc;

Two) pharmaceutical company- where objectives can be aimed at finding the therapeutic window and an optimal schedule;

Three) scientific setting- where different and sometimes esoteric objectives can be aimed at.

For any such case, certain fitness function can be formulated, reflecting all given requirements. Thus, in any particular case one can compare between different protocols and obtain the most suitable to his/her special purposes and needs.

Using the fitness function we can: a) estimate the efficacy of a given protocol, b) search for the solution of an optimization problem, that is predict which protocol will be best of many potential protocols considered for curing/relieving the patient.

7

6. Solving the Optimization Problem

The optimization problem is stated using the described models: to find the protocol for drug administration (with option to growth factor administration) which maximizes the given fitness function.

As explained above, we define the fitness function according to the user requirements. For example, the goal of the treatment may be defined as minimizing the number of cancer cells at the end of the treatment, minimizing the damage to the BM cells throughout the treatment or at its end, and curing the patient (where cure is defined precisely) as quickly as possible. Note that the fitness function may also include goals such as maximizing life expectancy, minimizing cost of treatment, etc.

Generally, the aim of optimization is to find the best protocol, i.e. the protocol that generates the best value of fitness. Customarily, this is achieved by mathematical analysis. However, mathematical analysis is restricted to relatively simple models, whereas our models are very complex and, therefore, cannot be solved analytically. On the other hand, the practical purpose of the treatment is not to find *the best possible protocol* (i.e., the global optimum) but "only" one that will suit the user's objectives, even if its fitness is not absolutely the best (i.e., the local optimum). For this reason we can be satisfied with the solution that can be shown to promise that the patient will be cured.

Hence, the optimization problem may be reformulated as follows: for given starting conditions, find the treatment protocol that will fulfill the user's requirements (e.g. curing a patient according to given definitions of cure) and subjected to given limitations (e.g. treatment duration, drug amounts, etc.). To this end it is unnecessary to find **the** global solution. It is enough to perform search, using search algorithms, in certain regions of the protocols' space, and find the local maxima of the fitness function. After determining these locally best protocols, we can verify that they serve one's objectives and check them numerically for stability.

Such a strategy can be used for identifying patient-specific treatment, as well as in the general case, where only the profile of the disease and the drug specified. If more patient-specific data are supplied, the solution will be tailored more specifically. On the other hand, the optimization program could propose general recommendations for the protocol types for certain kinds of tumor.